JAERI-M
92-191

CALCULATION OF NEUTRON FIELD GENERATED AT THICK Li TARGET BOMBARDED WITH 10-40 MEV DEUTERONS FOR ENERGY SELECTIVE NEUTRON IRRADIATION TEST FACILITY

December 1992

Yukio OYAMA, Seiya YAMAGUCHI*, Kazuaki KOSAKO**
and Hiroshi MAEKAWA

日本原子力研究所
Japan Atomic Energy Research Institute

JAERI-Mレポートは，日本原子力研究所が不定期に公刊している研究報告書です。
入手の問合わせは，日本原子力研究所技術情報部情報資料課（〒319-11 茨城県那珂郡東海村）あて，お申しこみください。なお，このほかに財団法人原子力弘済会資料センター（〒319-11 茨城県那珂郡東海村日本原子力研究所内）で複写による実費領布をおこなっております。

JAERI-M reports are issued irregularly.
Inquiries about availability of the reports should be addressed to Information Division Department of Technical Information, Japan Atomic Energy Research Institute, Tokaimura, Naka-gun, Ibaraki-ken 319-11, Japan.

編集兼発行　日本原子力研究所
印　　刷　ニッセイエブロ株式会社

JAERI-M 92-191

Calculation of Neutron Field Generated at Thick Li Target Bombarded with 10-40 MeV Deuterons for Energy Selective Neutron Irradiation Test Facility

Yukio OYAMA, Seiya YAMAGUCHI*, Kazuaki KOSAKO**
and Hiroshi MAEKAWA

Department of Reactor Engineering
Tokai Research Establishment
Japan Atomic Energy Research Institute
Tokai-mura, Naka-gun, Ibaraki-ken

(Received November 9, 1992)

Characteristics of neutrons generated from the lithium target bombarded with high energetic deuterons of 10-40 MeV have been calculated to determine the specification for the neutron irradiation material test facility (ESNIT) planned at Japan Atomic Energy Research Institute. The simple nuclear reaction model was applied to estimation of neutron flux distribution and energy spectrum and the results showed an agreement with the reported experiment within a factor of 2. The present calculation gives the basic spectrum data for estimation of damage parameters in test samples to evaluate the high energy neutron effect on them.

Keywords: D-Li Neutron Source, Neutron Flux Distribution, Stripping Reaction, Evapolation, High Energy Neutron, Material Research, ESNIT

---

* National Laboratory for High Energy Physics

** Nuclear Energy Data Center

エネルギー選択型中性子照射試験施設に用いる 10-40MeV重陽子で照射した 厚いリチウム・ターゲットから発生する中性子場の計算

日本原子力研究所東海研究所原子炉工学部
大山　幸夫・山口　誠哉*・小迫　和明**・前川　　洋

(1992年11月9日受理)

10から40MeVの高エネルギー重陽子を厚いリチウム・ターゲットに照射した時に発生する中性子場の特性を、原研で計画されている材料照射用中性子源（ESNIT）の仕様を決定する際の参考とするためにモデル計算を行った。簡単な核反応モデルを用い、ターゲット周辺での中性子束分布とエネルギースペクトルを求めた。計算結果は報告されている実験値とファクター2の範囲で一致した。この計算結果は高エネルギー中性子による材料損傷パラメーターへの効果を調べるために用いられる。

東海研究所：〒319-11　茨城県那珂郡東海村白方字白根2－4
＊　　高エネルギー研究所
＊＊　㈱原子力データセンター

Contents

目　　次

1. INTRODUCTION

Energy Selective Neutron Irradiation Test Facilty (ESNIT) to use for material research in a fusion reactor is planned at Japan Atomic Energy Research Institute .[1,2] To obtain various neutron flux spectra, a deuteron-lithium reaction neutron source is proposed for the high energy neutron irradiation facility with capability of deuteron energy selection. In damage processes due to the neutron irradiation, the variation of neutron energy causes changes to the damage parameters such as PKA (primary knock-on atoms) energy, the amount of displacement (dpa), electronic energy loss and nuclear transmutation products. Such changes to the damage parameters lead to the neutron energy dependence of radiation damage and irradiation effects. Therefore the energy selectivity is very attractive to study the damage phenomenon depending on neutron energy. The requirements for the neutron irradiation field for such material studies are summarized in Ref. 1 as follows: 1) maximum flux of more than 1.5-3 x 10^{14} n/cm^{2}s (10-20 dpa for stainless steel), 2) irradiation volume of more than 125 cm^3 with the neutron flux above 1.5 x 10^{14}, 3) flux gradient less than 10% and 4) more than three peak energy adjustments.

A deuteron-lithium (D-Li) reaction source was extensively discussed for 35 MeV deuteron energy case in the earlier work of the neutron irradiation material research facility such as the FMIT program.[3] The ESNIT concept, however, incorporates deuteron energy selection in order to vary neutron energy spectra. Parametric neutronic calculations are necessary for various incident deuteron energy to optimize the design of deuteron beam profile and specification and to study the sensitivity of netron spectrum obtained from the D-Li source to the damage parameters. In addition, the source neutron condition influences the neutron shielding design to construct such a facility.

The calculations mentioned above basically require the double differential ^{7}Li(d,n) reaction cross section as a function of deuteron energy. But the experimental data[4-6] obtained so far seems to be inconsistent with each other and then not adequate for the present purpose. Hence, we adopted a simple theoretical model of the cross section so as to perform the above neutronic calculations in a certain degree of accuarcy and to overlook the characteristics of such facility. In this paper, simplified nuclear model adopted for neutron production reaction and calculation method for neutron flux distribution in irradiation field are described. And the characteristics of neutron field with and without test material are discussed.

2. CALCULATION METHOD

2.1 Neutron Spectrum near the Target

Since the accelerated deuterons slow down in the lithium layer due to ionization energy loss, the reaction energy with lithium is changed as the deuteron goes through the trajectry in the lithium. This provides distributed source as a function of the depth inside of the lithium target as shown in Fig. 2.1. Representing the reaction point as (x',y',z'), where z' denotes beam direction, the neutron source strength S with energy E_n and angle Θ for the incident deuteron energy E_d is given by the following equation in a laboratory system.

$$S(x',y',z';E_n,\Theta) = \frac{N \cdot J}{e} \left(\frac{d^2\sigma}{d\Omega dE_n}\right)_{CM} \cdot \left|\frac{\partial(\Omega_c,E_{nc})}{\partial(\Omega_L,E_{nL})}\right| \qquad (2.1)$$

$$[n/(sr \cdot s \cdot MeV \cdot cm^3)],$$

where N is the density of Li atom and J = J(x',y'), the deuteron current density profile, e is the unit charge, $(d^2\sigma/d\Omega dE_n)_{CM}$ is the double differential cross section of neutron production in a center of mass system and the last term is Jacobian for the frame transformation from the center of mass to the laboratory systems. This relation can be formulated by relativistic kinematics. (See Appendix 1) The Li(d,n) cross section is given later by a simple nuclear reaction model.

To obtain the neutron flux spectrum at the point (x,y,z) in irradiation space in front of the target, neutron source distribution S is integrated over the source region (x',y',z') with a relationship of $1/r^2$ to the point (x,y,z) as shown in Fig. 2.2.

$$\Phi(\vec{r},E_n) = \int_{\substack{\text{source} \\ \text{volume}}} \frac{S(\vec{r}';E_d;E_n)}{|\vec{r}-\vec{r}'|^2} \cdot d\vec{r}' \ , \qquad [n/(s \cdot cm^2 \cdot MeV)] \qquad (2.2)$$

Assuming that the attenuation of deuteron flux through the range is negligible, the integration through the trajectory can be transformed to the integration by deuteron energy using stopping power. Here we replace the integration with respect to z' by the deuteron energy which can be related to the depth z' by using the stopping power.

To simplify the integration, we assume cylindrical symmetry and introduce cylindrical coordinates (r',θ') in stead of (x',y'), and then J=J(r). Finally, we calculate as follows:

$$\Phi(\vec{r},E_n) = \int \frac{S(\vec{r}';E_n,\Theta)}{|\vec{r}-\vec{r}'|^2} \frac{1}{(dE_d/dX)} dr'd\theta'dE_d \ , \qquad (2.3)$$

where (dE_d/dX) is the stopping power. The stopping power is represented for the incident energy range of 1-100 MeV as the following formula given in Ref. 9.

$$\left(\frac{dE_d}{dX}\right) = \left(A_6/\beta^2\right)\left[\ln\left(\frac{A_7\beta^2}{1-\beta^2}\right) - \beta^2 - \sum_{i=0}^{4} A_{i+8}(\ln E_d)^i\right]$$

$$[eV/(10^{15}atoms/cm^2)] \qquad (2.4)$$

where E_d = deuteron energy/deuteron mass [keV/amu], β = v/c and A_i is given for lithium in the table of Ref. 9 as A_6=0.00153, A_7=21470, A_8=-0.5831, A_9=0.562, A_{10}=-0.1183, A_{11}=0.009298 and A_{12}=-0.000166, respectively. Figure 2.3 shows the relation between the depth and deuteron energy calculated for 40 MeV deuterons in lithium. One can see that the relation in the region of 20-40 MeV is almost linear, and the reactions below 20 MeV take place in the last 6 mm. The stopping power also gives energy deposition rate in the material, i.e., a heat deposition profile as shown in Fig. 2.4.

2.2 Nuclear Reaction Model

The differential cross section is calculated by the same assumption as that of Johnson et al.,[3] except some modifications. The neutron production reaction of ^{7}Li(d,n)^{8}Be is only considered for the main reaction among the possible reactions shown in Table 2.1, and in the calculation of cross sections the Serber's stripping reaction model[4] and the evaporation process are taken into account by the following linear combination.

$$\left(\frac{d^2\sigma}{d\Omega dE_n}\right) = A_S\left(\frac{d^2\sigma}{d\Omega dE_n}\right)_{Serber} + A_C\left(\frac{d^2\sigma}{d\Omega dE_n}\right)_{Evapolation} , \qquad (2.5)$$

The first term by the Serber's theory is written as follows:

$$\left(\frac{d^2\sigma}{d\Omega dE_n}\right)_{Serber} = \frac{1}{2} \frac{(E_d-E_b)\cdot E_b}{\left[(E_n-E_d/2)^2 + E_b\cdot E_d\right]^{3/2}} \cdot \frac{\Theta_0}{\left(\Theta_0^2+\Theta^2\right)^{3/2}} \quad \text{for } |E_n-E_d/2| < 2(\Delta E)_{1/2}$$

$$= 0 \quad \text{for } |E_n-E_d/2| \geq 2(\Delta E)_{1/2} \qquad (2.6)$$

where E_d : Incident deuteron energy,

E_b : Binding energy of deuteron,

Θ_0 : $\sqrt{E_b/E_d}$.

And the second term of evaporation process is due to compound reaction:

$$\left(\frac{d^2\sigma}{d\Omega dE_n}\right)_{Evapolation} = E_n \cdot e^{(-E_n/T)}, \qquad (2.7)$$

where T : $3.2\sqrt{E_d/A}$ (A:mass number).

Here we modified the Serber's cross section by adding the energy cut-off ($E_c = E_d/2 \pm$ FWHM , full-width-half-maximum) for the neutron spectrum tail by Eq. (2.6), because the high energy tail of Serber's spectrum breaks an energy conservation law and that model may be valid only for a gross structure. This energy cut-off, however, can not eliminate producing the negative energy neutrons in lower energy tail by this model. This may provide the unreasonable increase of the lower energy neutrons below ~2 MeV, and also the break-up reactions to two or three bodies should be taken into account for low energy range. Hence this modification is not valid for such low energy region. The other type of reaction is also necessary to be considered for the higher energy neutrons above E_d; Q-value of 15 MeV means there is a possibility for generating the high energetic neutrons of E_d+15 MeV to the ground state of residual nuclei. Since this is not considered here, higher energy neutrons are produced only as an evaporation tail.

The A_s and A_c are energy dependent mixing parameters of two spectral shapes. The energy cut-off of 6 MeV for A_s comes from the low energy limit of stripping reaction for ^{7}Li. The shoulder of 10 MeV was introduced as an energy-weighting parameter but it was insensitive. The parameter A_c was weighted for lower energy deuterons shown in Fig.2.5. The energy cut-off of 2 MeV for the energy of coulomb varier and the high energy cut-off of 15 MeV for energy weighting parameter were introduced for A_c. The values of parameters in A_s and A_c were determined by the trial and error method to reproduce the measured spectrum and angular distribution. The evaporation part is essentially needed for representing the angular distribution.

2.3 Comparison with the Experiments

The present source model was confirmed by comparison with the experimental data for a thick lithium target. These measurements correspond to the spectrum at the place far away from the target, because those experimental setup were performed at least 2 meters away from the target. For this geometry, we can assume the target is a point, and then the observed spectrum is written simply as follows:

$$\Phi(E_n,\Theta) = \frac{N \cdot J}{e} \int_{E_0}^{0} \left(\frac{d^2\sigma}{d\Omega dE_n}\right)_{CM} \cdot \frac{1}{(dE_d/dx)} \cdot \left|\frac{\partial(\Omega_c, E_{nc})}{\partial(\Omega_L, E_{nL})}\right| dE_d \qquad (2.8)$$

The spectra at 0 degree calculated by the above equation are shown in Fig. 2.6 for various incident energy for deuterons. It is clearly seen that the peak energy is shifted with decrease of deuteron

energy and the peak energy corresponds closely to the half of deuteron energy; the peak energy shifts 4 MeV to 15 MeV corresponding to the incident deuteron energy of 10 to 40 MeV. This wide energy range is the merit of the energy selective neutron irradiation facility (ESNIT). The neutron spectrum by 40 MeV deuterons has the peak closed to the D-T reaction neutrons, but the spectrum is broadened spread over 30 MeV. The spectrum with a 4 MeV peak obtained by 10 MeV deuterons has few neutrons above 10 MeV. Thus a study by combination of neutron irradiation with these spectra will give energy dependent effects of neutron irradiation damage on test materials.

Figure 2.7 shows the comparison of the calculated spectra for 0 degree by Eq. (2.8) with the measured ones.[6,7] The present calculations agree well with the Lone's data[5] for 23 MeV and with the Weaver's data[6] for 18 MeV, but are inconsistent with the Goland's data.[7] In Fig. 2.8, the spectrum for 35 MeV case is compared with the data by Johnson. et al. for various angles.[3] One can see from the very high energy part of the spectrum measured in UC-DAVIS that there exist a peak around 45 MeV corresponding to neutron emissions to the levels of ^{8}Be below 15 MeV. At the energy of 45 MeV, the measured flux is 100 times larger than that of this calculation, but 100 times smaller than the flux around 15 MeV. Below 40 MeV the difference is smaller especially at forward direction by a factor of 2 and the agreement at the large angles is within a factor of 2-3.

The 0-degree neutron emission yield for the energy integrated spectrum above 2 MeV is also compared with the experimental curve summarized by Lone[8] as shown in Fig. 2.9. The calculation was normalized to this experimental curve at 35 MeV. It can be seen that the relative energy dependence of the calculation shows fairly good agreement.

The angular dependence of neutron emission by the present calculation, shown in Fig. 2.10, agrees fairly well with the experiment for high energy deuteron, but for lower energy the flux at large angle is slightly larger. This is consistent with the large evaporation value for low energy deuteron in the model as seen in Fig.2.6. However this is not serious discrepancy because most of the contribution to the irradiation field comes from the forward emission in which the agreement is enough.

Table 2.1 Neutron producution channels and Q values for d-Li reaction

Target	Reaction	Q (MeV)
^{7}Li	(d,n)^{8}Be	+ 15.0
	(d,2n)^{7}Be	- 3.9
	(d,3n)^{6}Be	- 14.5
	(d,pn)^{7}Li	- 2.2
	(d,α)^{5}He	+ 14.2

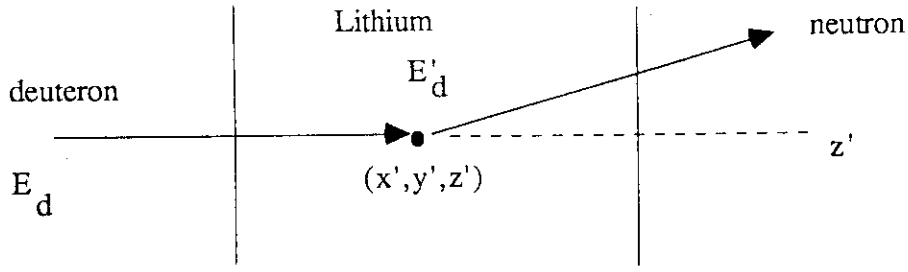

Fig. 2.1 Deuteron reaction inside of the lithium target.

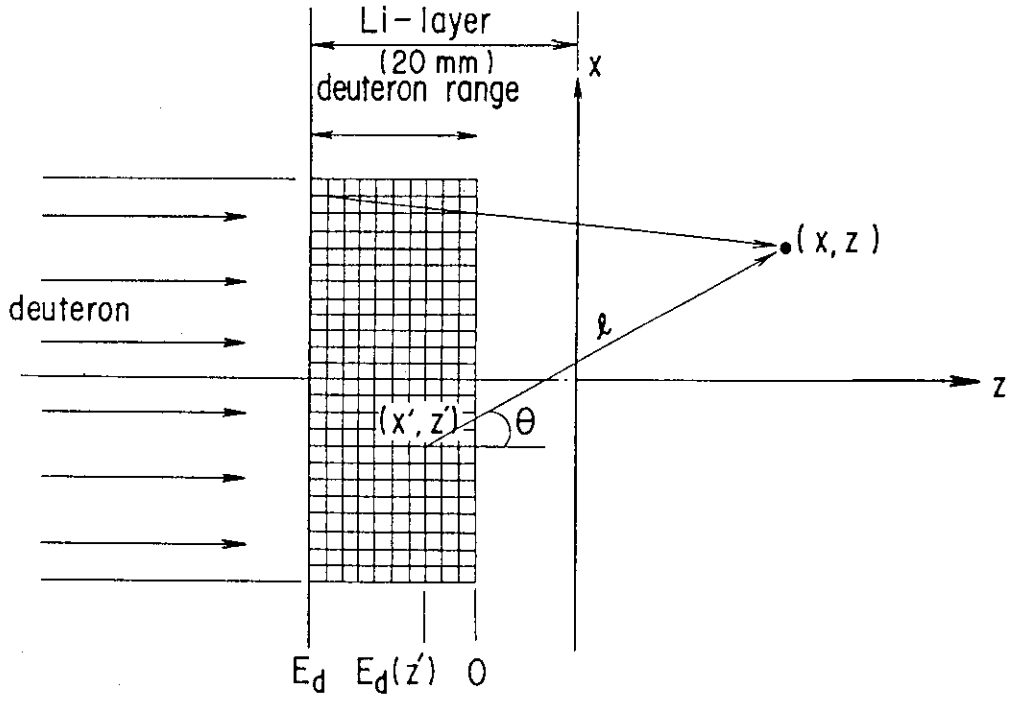

Fig. 2.2 Calculation model for neutron flux distribution in the irradiation space.

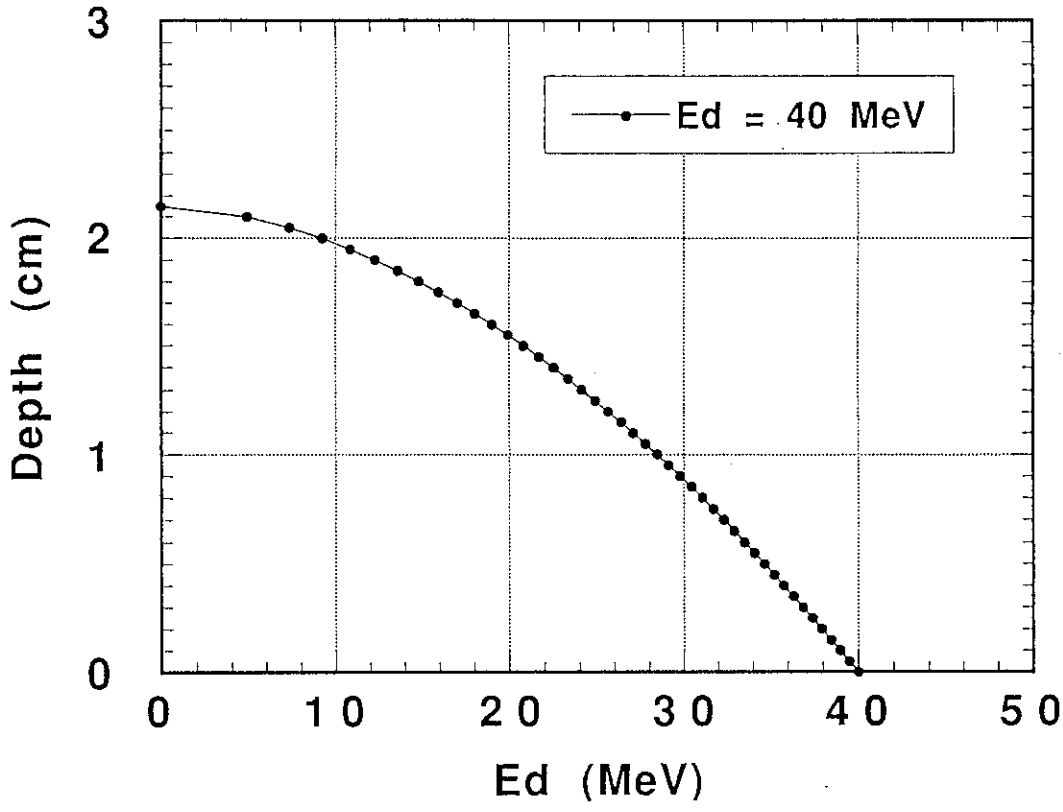

Fig. 2.3 Relation of the depth in lithium vs. the deuteron energy for the 40 MeV incident energy.

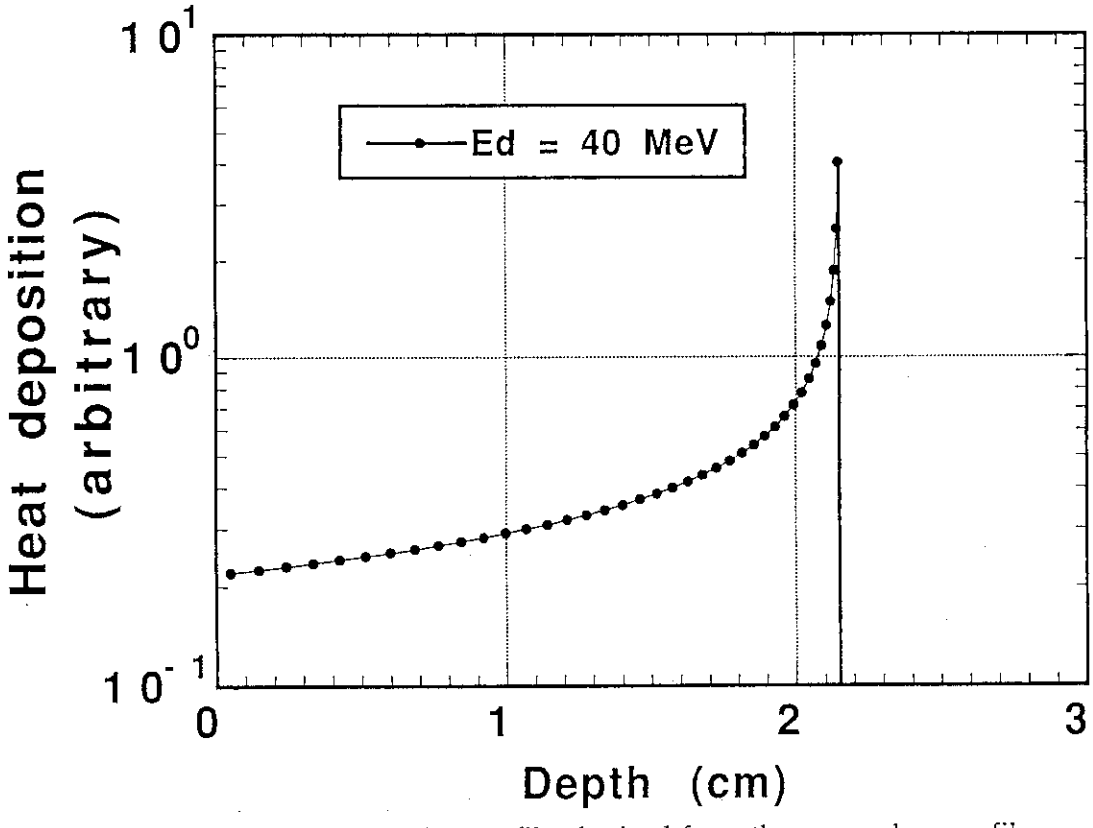

Fig. 2.4 Heat deposion profile obtained from the energy loss profile.

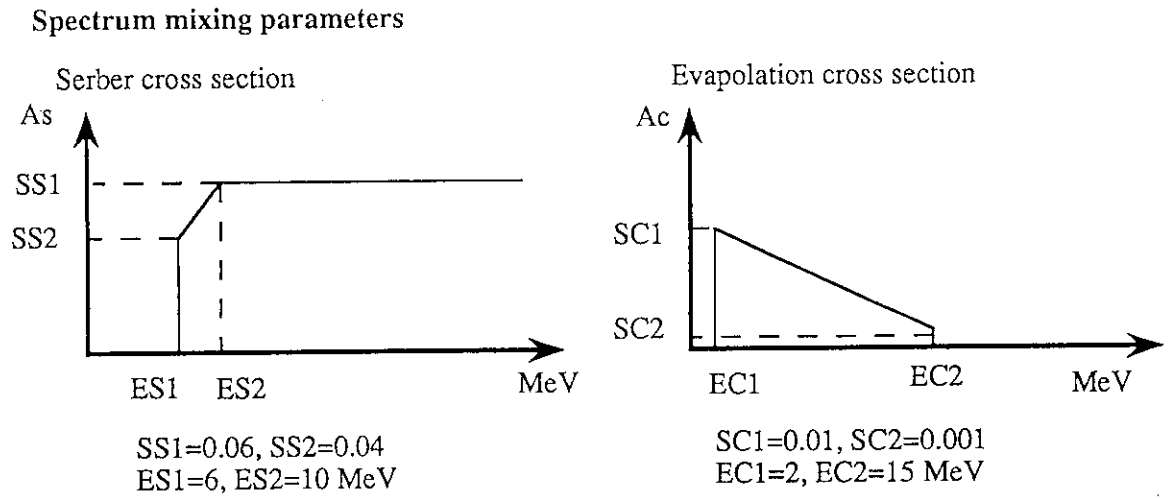

Fig. 2.5 Energy dependence adopted for mixing parameters of two spectra.

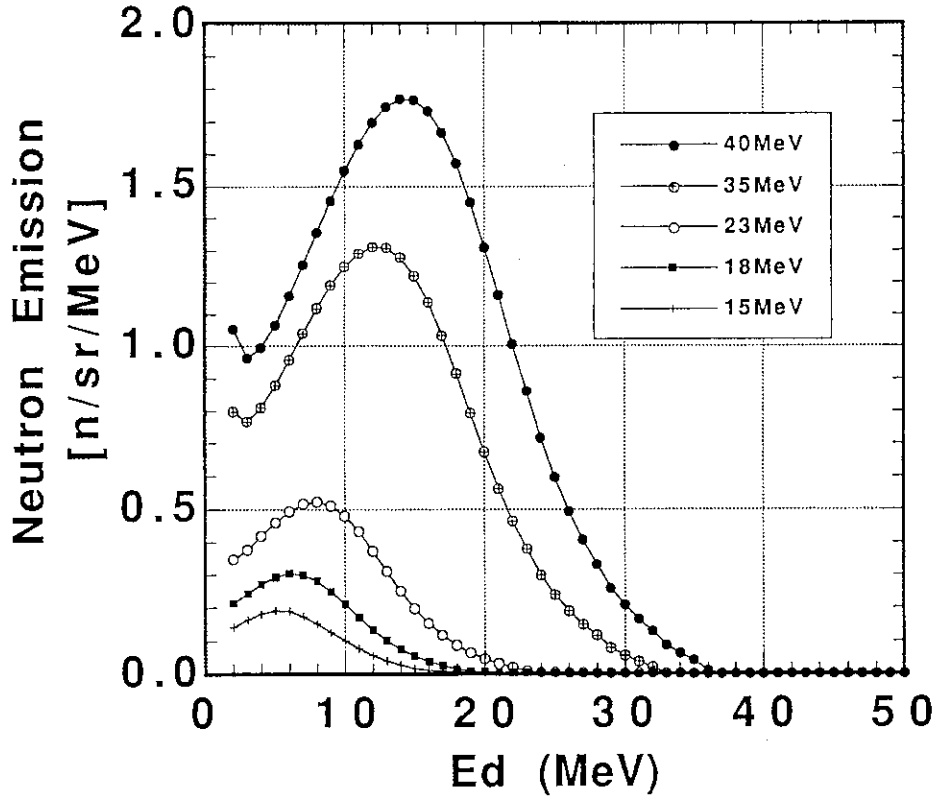

Fig. 2.6 Calculated neutron energy spectrum at forward for various deuteron energies.

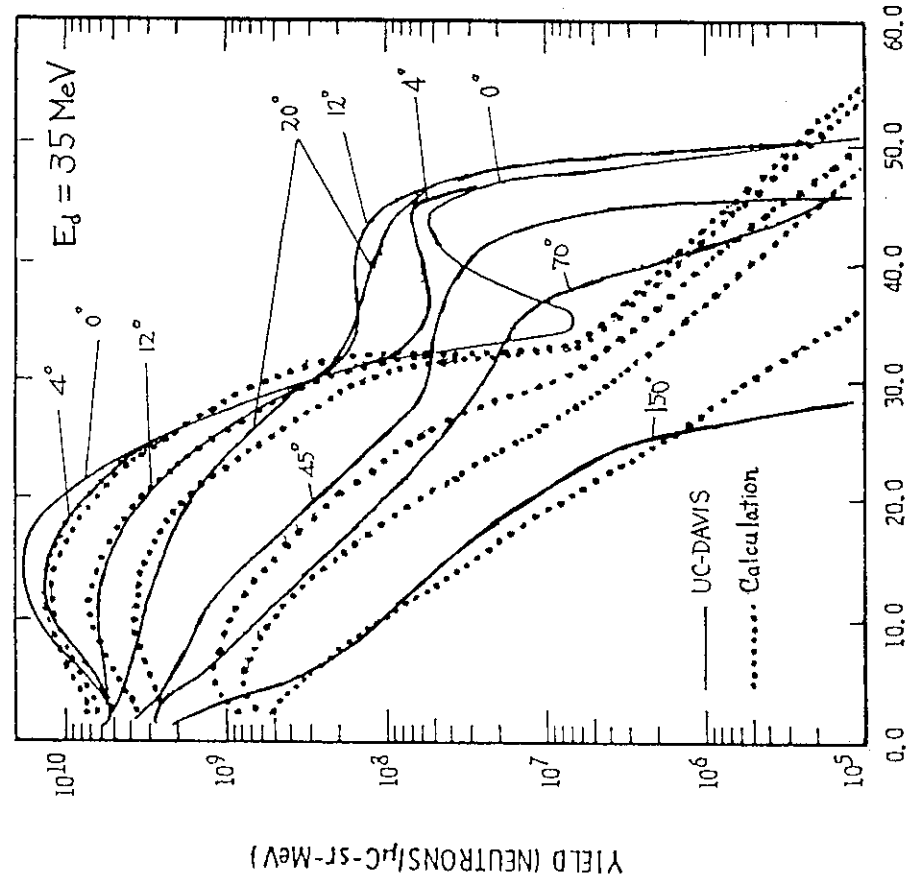

Fig. 2.7 Comparison of the calculated neutron spectra with the measured ones for different energies.

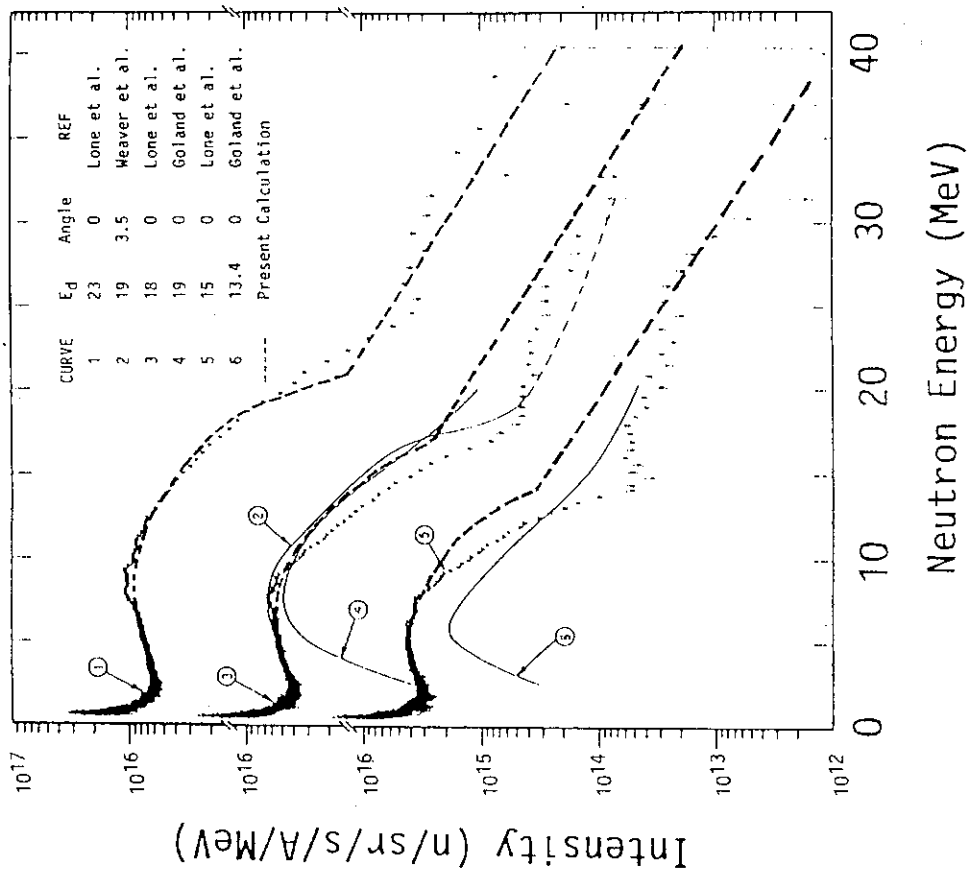

Fig. 2.8 Comparison of the calculated neutron spectra for 35 MeV with the measured one at various angles. The experiment was performed at UC-DAVIS.[4]

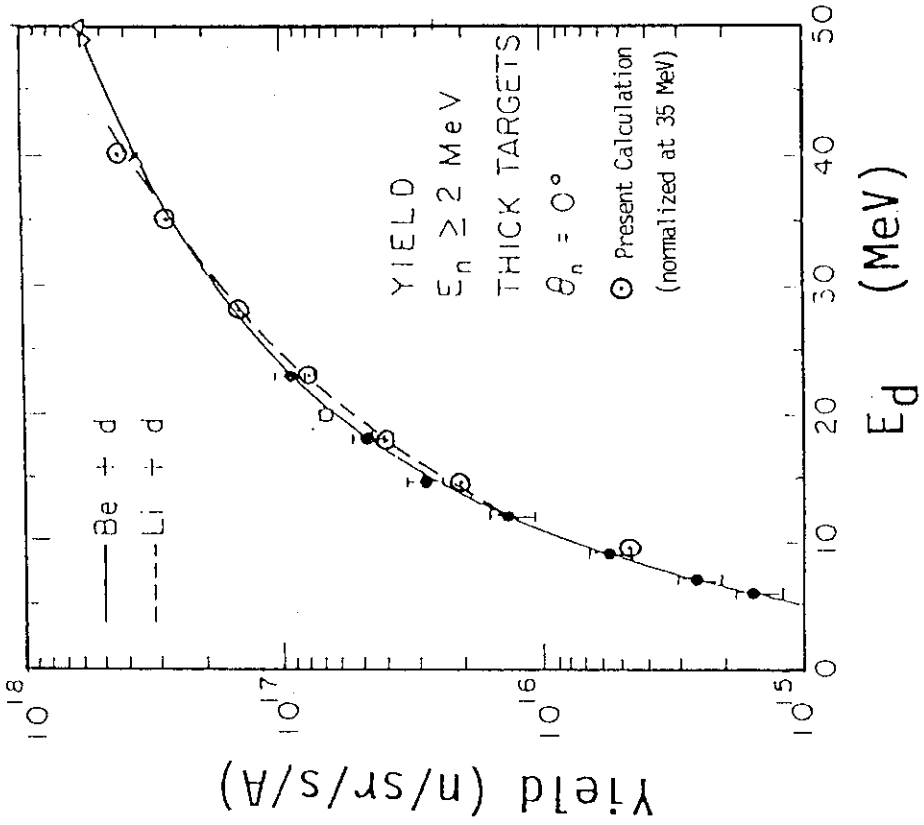

Fig. 2.9 Comparison of energy dependence of the incident deuteron on the 0-degree neutron yield for a thick Li target.

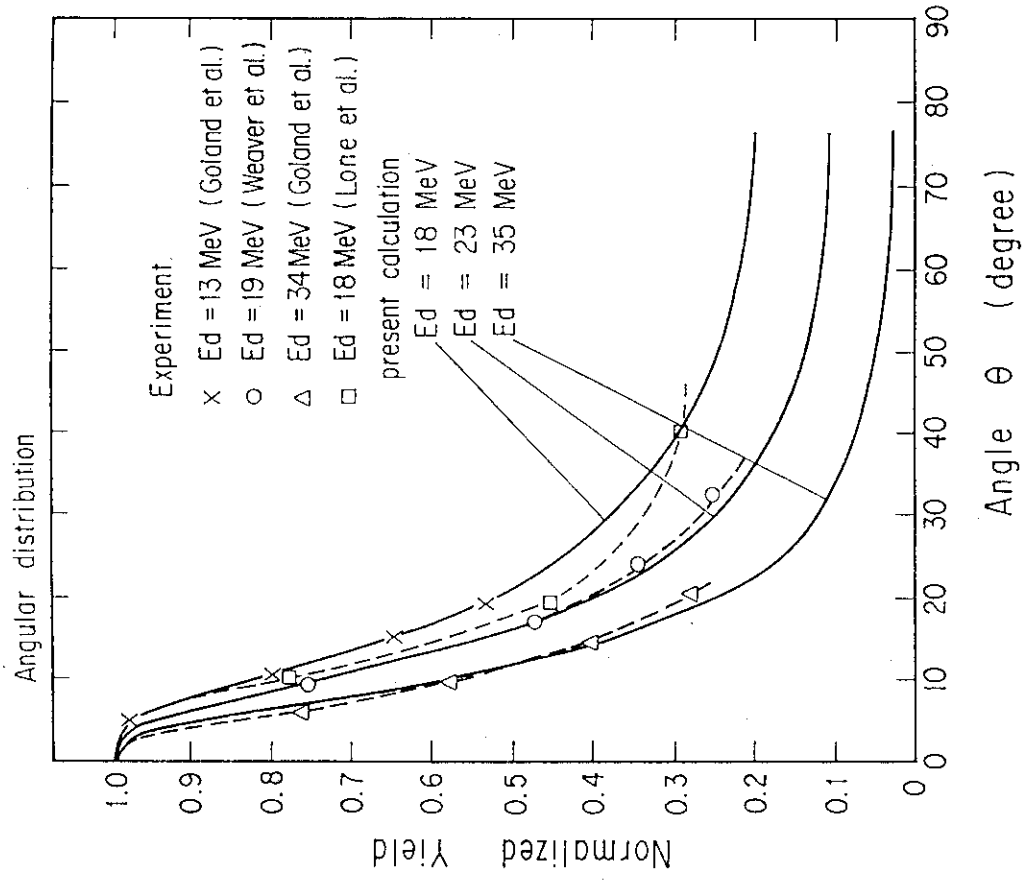

Fig. 2.10 Angular distribution of neutron emission from the target.

3. CHARACTERISTICS OF NEUTRON IRRADIATION FIELD

3.1 Neutron Spectrum

Since the range of deuteron in lithium is about 16 mm for 35 MeV and 21 mm for 40 MeV, respectively, the thickness of lithium target should be more than 22 mm for the 40 MeV case. The neutron flux at the place was estimated by the uncollided flux. The neutron scatterings by the lithium and the thin target backing material were neglected in the calculation, because the forward contribution of the scatterings will be a few % by inference from the D-T reaction neutron case.

Neutron source distribution along the deuteron range has to be considered for neutron spectrum calculation at the place very close to the target. When the neutron field near the target is used as neutron irradiation space, the distance from the reaction position to the irradiation point varies with the deuteron energy corresponding to the energy loss. This means the neutron flux spectra from the positions closer to the sample , i.e., at the deeper positions in the range, are contributed larger than the spectra at the higher energy deuteron on the lithium surface due to the $1/r^2$ effect. Thus the neutron spectrum at the position close to the target is sensitive to the depth because of deuteron reaction energy as mentioned in the previous section. This situation is shown in Fig. 3.1 for the case of 35 MeV deuterons at the positions of the surface just behind the lithium layer to the 50 mm distance from the surface along the 0 degree axis. One can see that the spectra shift to lower energy at the positions closer to the target. The peak energy at the surface is 6 MeV, while the peak energy at the position far away from the target is about 12 MeV. The change of spectrum shape saturates at the distance over 30 mm from the surface. For low energy deuterons, the spectrum change is small because of the shorter deuteron range. For example, the range of 18 MeV deuteron is 5 mm. This kind of spectrum shift is very important for the irradiation at the place very close to the target in which the highest neutron flux can be obtained.

3.2 Neutron Flux Distribution

Here we assume that deuteron current is 40 mA and the beam size is 20-40 mm in diameter. Since the ^{7}Li(d,n) reaction has a strong anisotropy of neutron emission, most of neutrons are emitted in the angles within 20 degree. The neutron flux distribution along the 0 degree axis shows almost the $1/r^2$ dependence. The distribution on the axis perpendicular to the 0 degree axis, however, is very steep due to strong anisotropy of emitted neutron by higher energy deuteron. The peak neutron flux above 2 MeV at the point just behind the target is about 1×10^{13} n/cm^2/s for deuterons above 35 MeV. The neutron flux decreases quickly with the distance from the central axis, i.e., to 1/10 at the 20 mm distance. This gradient becomes gentle with increase of the distance from the target.

The deuteron energy dependence of the neutron flux distribution is shown in Fig. 3.2 for three energies. The neutron flux distribution generated by 40 MeV and 40 mA deuterons with a homogeneous beam profile of 40 mm-diameter spot is very strong at the forward, while the flux distribution generated by 23 MeV deuterons are broader than that of 40 MeV deuterons. Moreover the peak flux intensity is different by three times between both neutron fields. The irradiation volumes for the material test can be estimated from Fig. 3.3 which plots the obtained irradiation volume versus the lower limit flux required for the various deuteron beam conditions.When the beam current increases by 25%, i.e., to 50 mA, the flux should be increased by 25% as plotted in a dotted line because the neutron yield is proportional to the current. Hence the required irradiation volume of more than 125 cm^3 with the flux level above 1.5 x 10^{14} $n/cm^2/s$ can be achieved by 50 mA for the 40 MeV deuteron.

The flux gradient less than 10% at the irradiation field is another design requirement. As mentioned before, the flux gradient at forward direction is dominated by the $1/r^2$ law, while the gradient in perpendicular direction can be improved by increasing the target area for the front position, e.g., from 20 to 40 mm diameters. Therefore the flux gradient is limited only by $1/r^2$ law. If one desires smaller gradient, one should go far from the target. The gradient is written as

$$\frac{d\Phi}{dr} \approx -2A \cdot r^{-3} \leq 0.1 \times \frac{A}{r^2},$$

then to get the gradient smaller than 10%, it is necessary that r > 20 cm. This is impossible to keep the flux above 1 x 10^{14} $n/cm^2/s$ by 50 mA beam. To resolve the steep gradient near the target, the utilization of deuteron beam with a ring beam profile seems to be attractive. This concept leads the ring source distribution at the target and the gradient inside the ring is expected to be improved. Figures 3.4 and 3.5 compare the flux contour maps for both cases of squared and ring shape beam profiles, respectively. In the case of tehring profile, the flux at the center decreased so that the flux gradient came to be modest. One can see the flat flux distribution around the front space of the target for the ring case. However, due to angular dependence of emission neutron energy spectrum as seen in Fig.2.8, the ring beam may give lower energy neutrons at the central region than those of the spot beam.

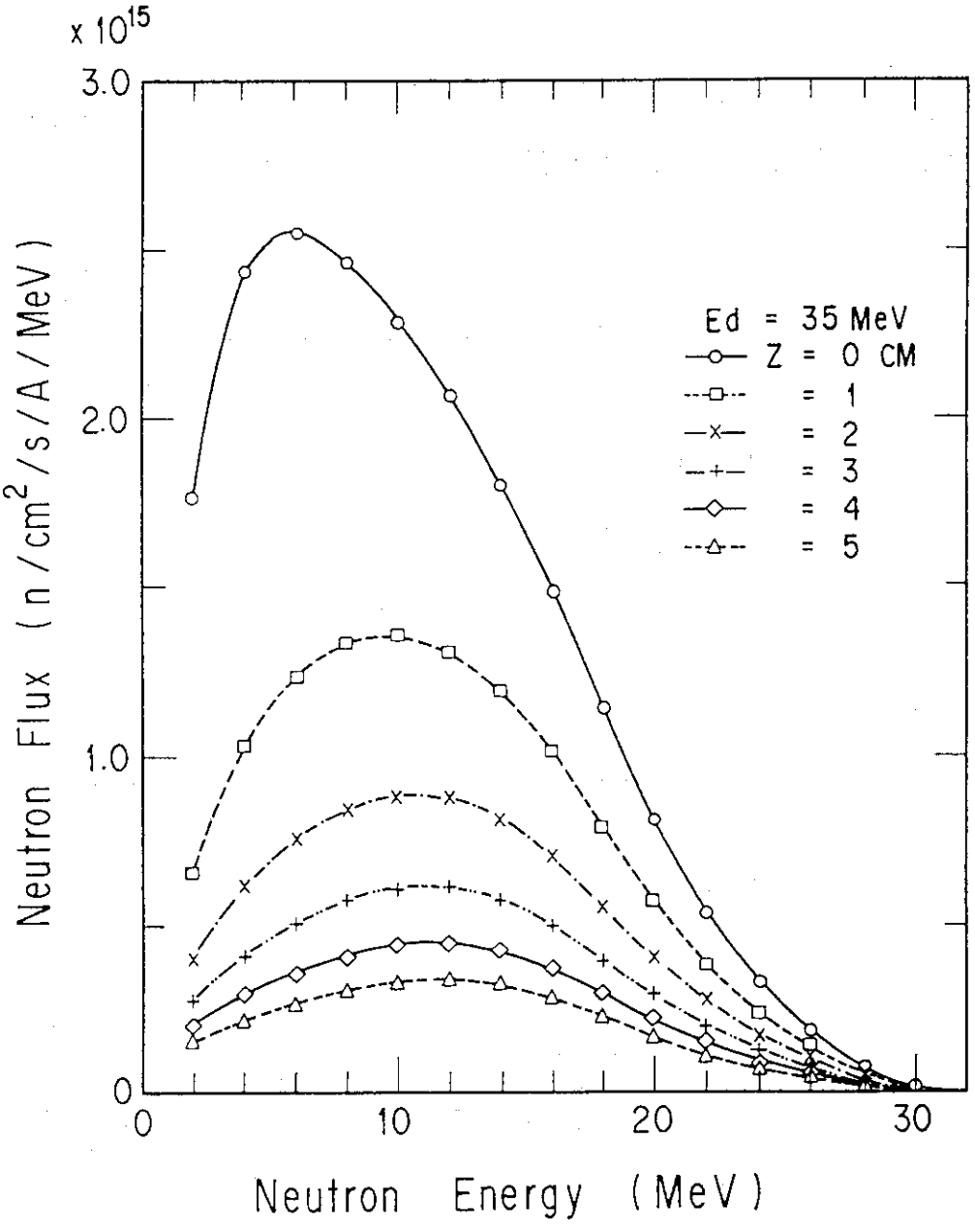

Fig. 3.1 Spectrum shape change with the distance from the target surface for 35 MeV deuterons.

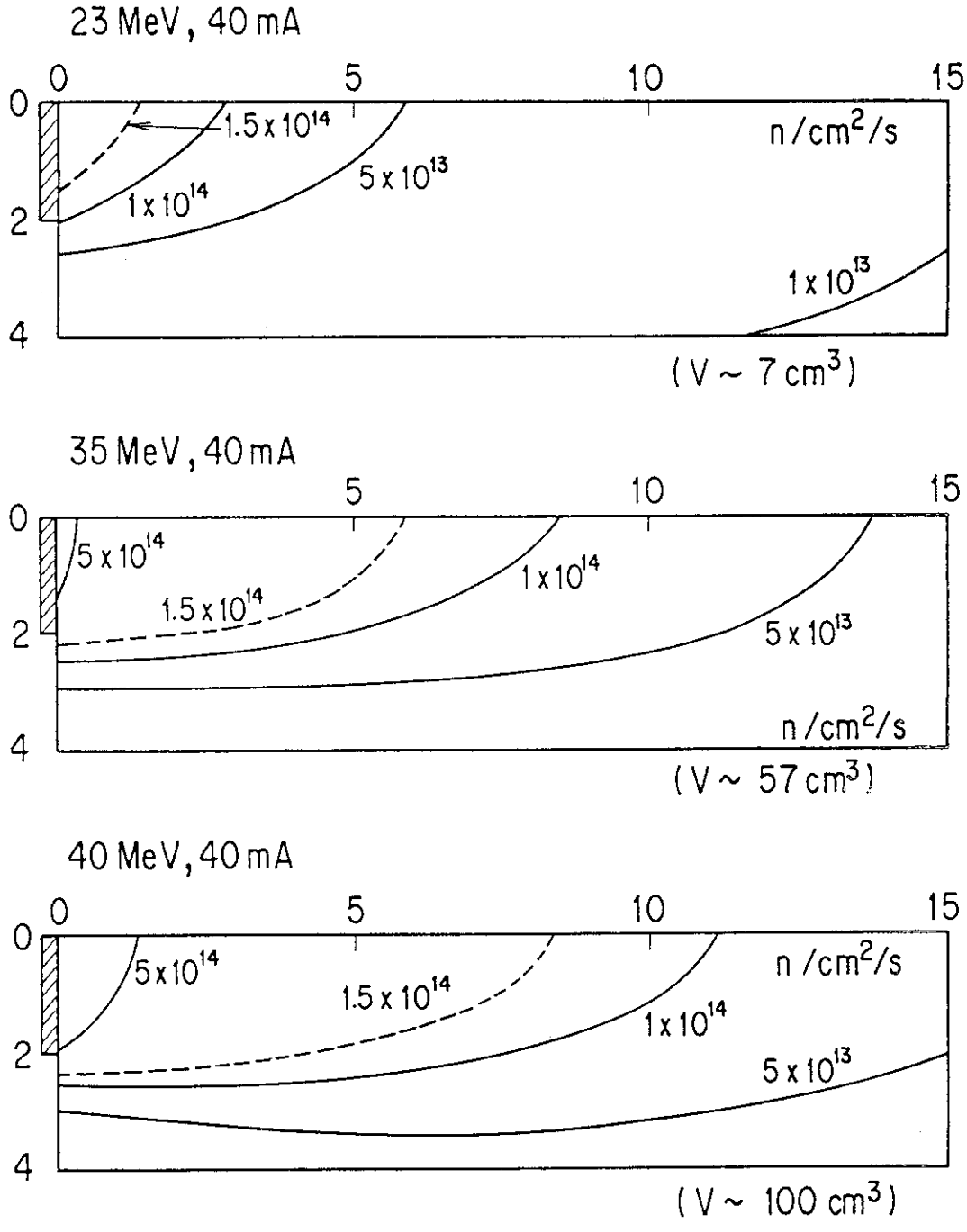

Fig. 3.2 Neutron flux contour map for various incident deuteron energies. (hatched part is the Li region)

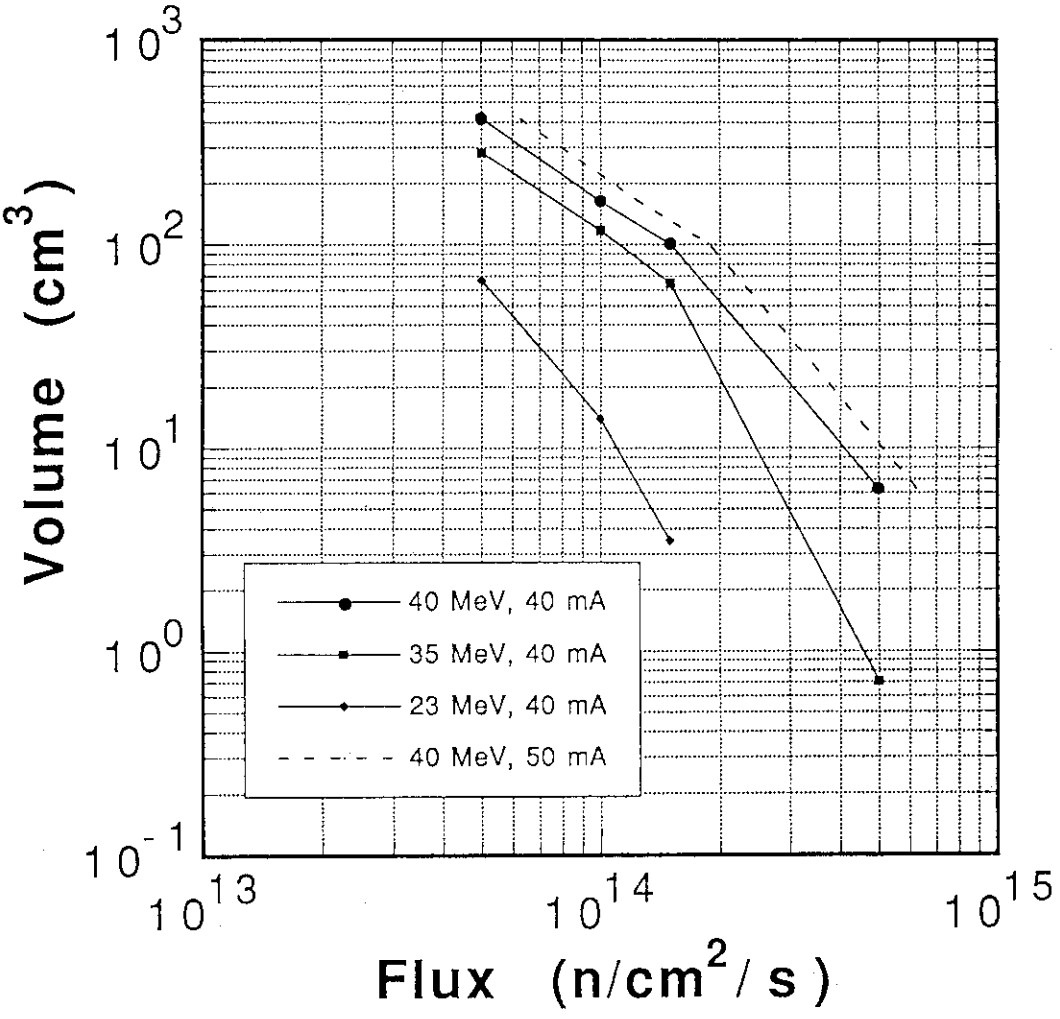

Fig. 3.3 Relation of irradiation volume and minimum flux with incident deuteron energy.

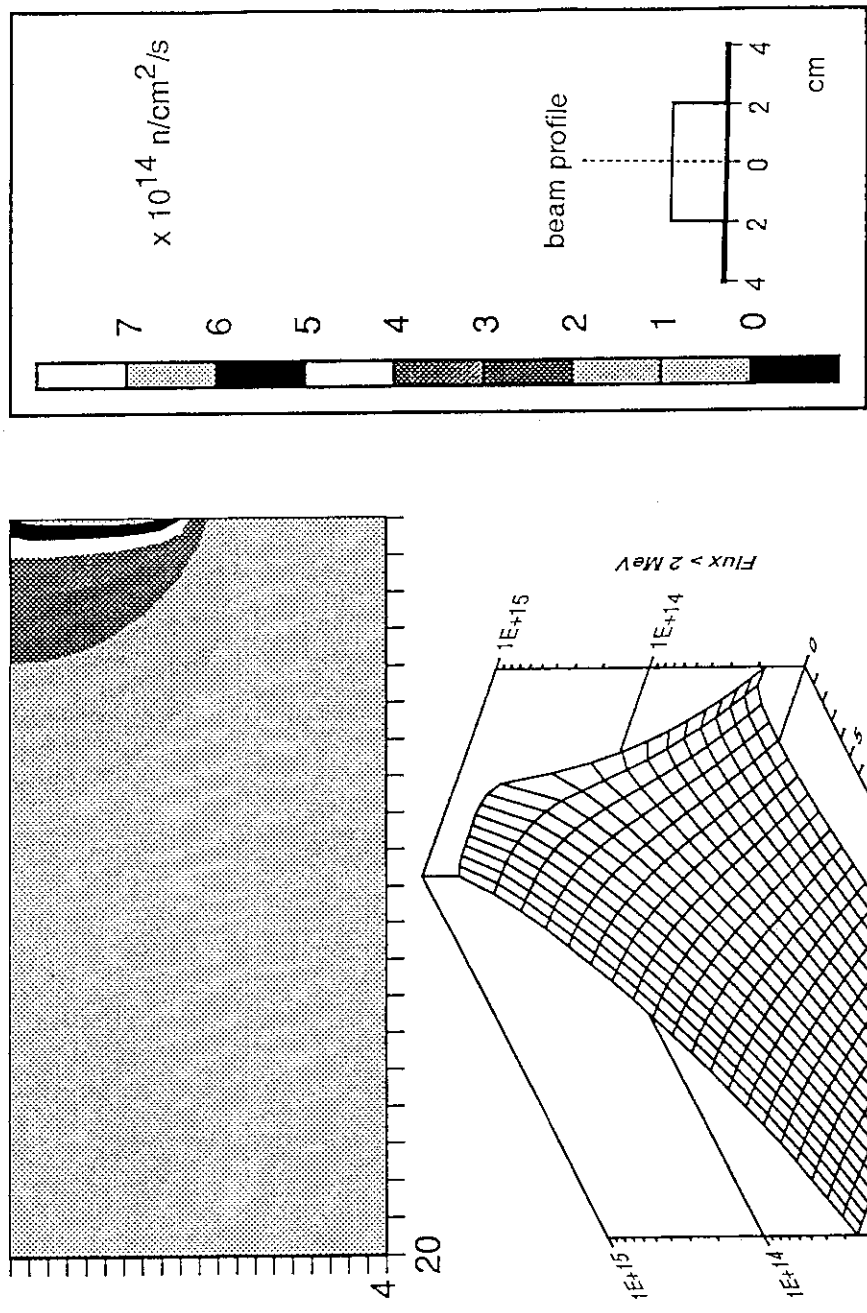

Fig. 3.4 Neutron flux distribution with a squared shape beam sopt for 40 MeV deuterons.

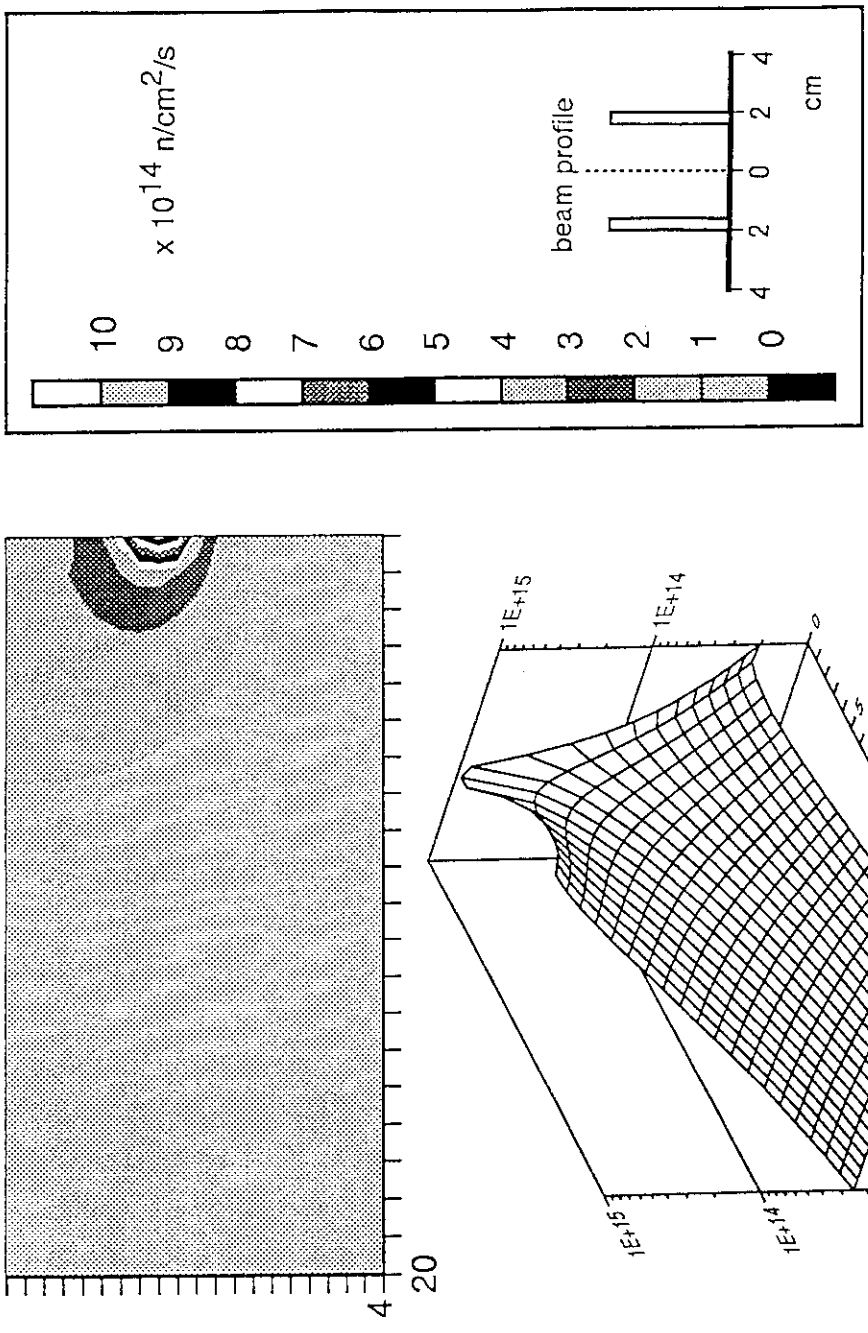

Fig. 3.5 Neutron flux distribution with a ring shape beam for 40 MeV deuterons.

4. CHARACTERISTICS OF NEUTRON FIELD IN TEST SAMPLES

In a practical neutron field for irradiation test, there exist a lot of scattered neutrons coming from the irradiation room wall and sample itself. Especially the scatterings in sample itself make a spectrum change of irradiation neutrons. Thus a neutron transport calculation was performed to obtain the neutron flux inside of the sample taking account for those scattered neutron components. For this calculation, the MORSE-CG[11] Monte Carlo neutron transport code and the DLC87/HILO[12] multigroup cross sections were used. The DLC87/HILO library has 66 neutron energy groups and 21 gamma-ray groups up to 400 MeV neutron energy with P_5 Legendre expansion at energies above 14.9 MeV and P_3 at energies below 14.9 MeV. The calculation model includes a irradiation room and a test material sample. For simplification the following model is adopted for all cases with 10, 23 and 40 MeV deuterons as shown in Fig. 4.1.

(1) The lithium target 20 mm is followed by 3 mm-thick stainless steel vacuum boundary.

(2) The source region is defined as 20 mm in diameter and 15 mm in thickness.

(3) The neutron source is homogeneously distributed in the source region and the source neutron energy spectrum and angular distribution are given by the tables calculated from Eq. (2.8).

These approximations are not valid for the locations near the target less than ~30 mm as discussed in Sec.3.1, but still useful for a quantitative discussion.

The irradiation room is 3 m x 4 m square and 3 m height surrounding by ordinary concrete wall as shown in Fig. 4.1. The target is set at the distance of 1.5 m from both walls. The test materials are chosen in iron and alumina with a cylinder of 50 mm in diameter and 80 mm in length placed at the 10 mm distance from the target chamber of stainless steel. The sample is divided in several cells for flux estimation as shown in Fig. 4.2. The details of model around the target is shown in Fig. 4.3.

Figure 4.4 shows comparison of the neutron spectra inside of the iron sample between with and without the room wall. Since the input source is given above 1 MeV because of limitation of the reaction model, there is a peak at 1 MeV due to this cut-off. The difference between both cases is very small and within the statistical errors in calculation. The difference is small even in thermal neutrons though those low energy neutrons are not shown. This is because the sample is placed very close to the target. Hence this indicates that it is not necessary to take care of room returned neutrons so much.

Figures 4.5 and 4.6 show the spectra at various locations inside of the iron and alumina samples for the 40 MeV deuteron case. The energy spectrum in the iron case decreases neutrons in the 6-8 MeV region with increase of the depth, while the spectrum in alumina flattens. One should note that the effective peak energy is shifted to higher energy in the iron case. Figures 4.7-4.9

show the spectra at the center of second layer (10-20 mm inside of the iron and alumina samples) for three different deuteron energies. It is seen that the spectrum for iron is larger than that of alumina below 4 MeV, but smaller at the 4-15 MeV and almost the same for higher energy part . It is noticed that the effective neutron peak energy is different form each other inside of samples with a few MeV.

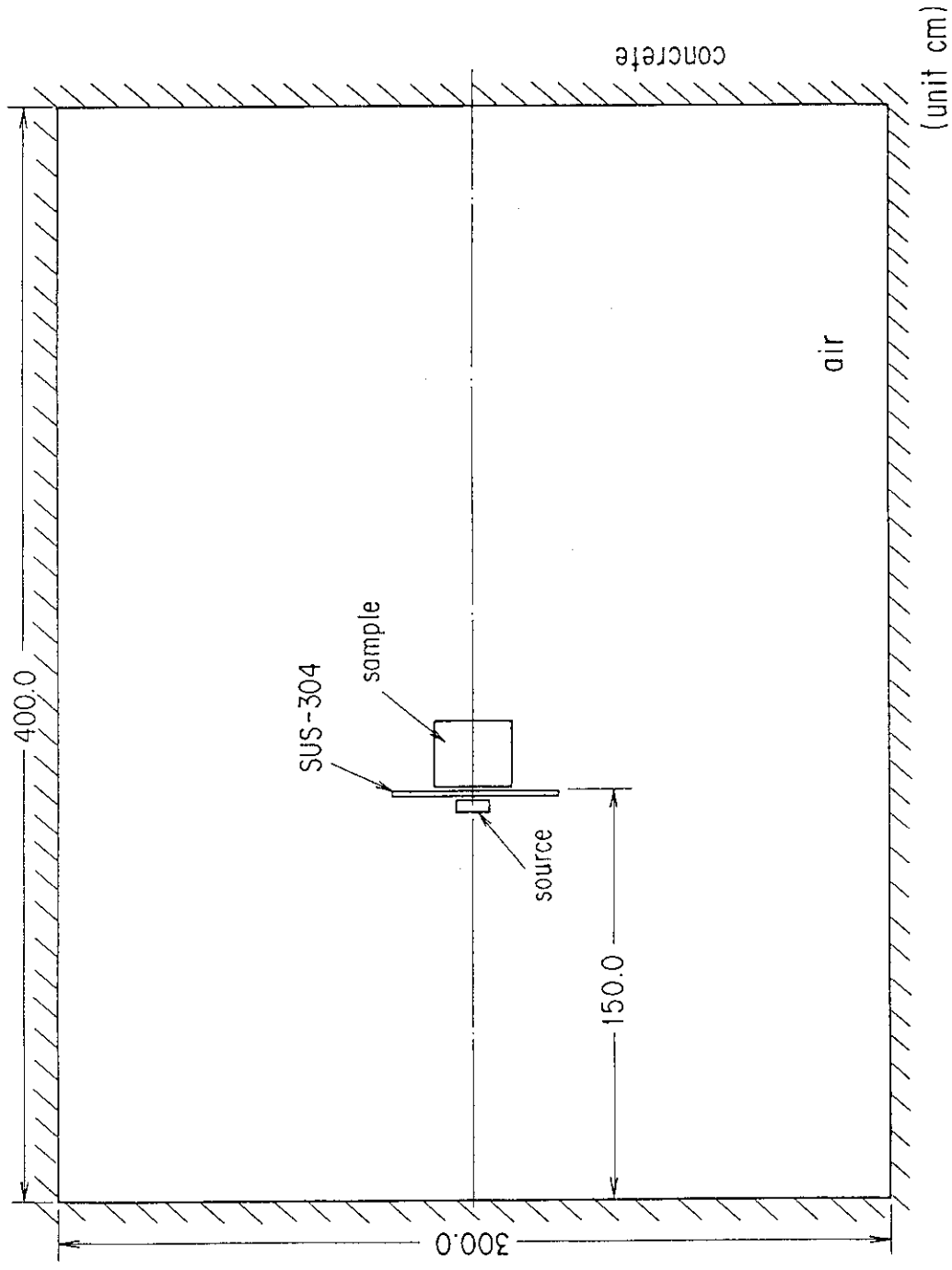

Fig. 4.1 Calculation model for irradiation room, lithium target and sample.

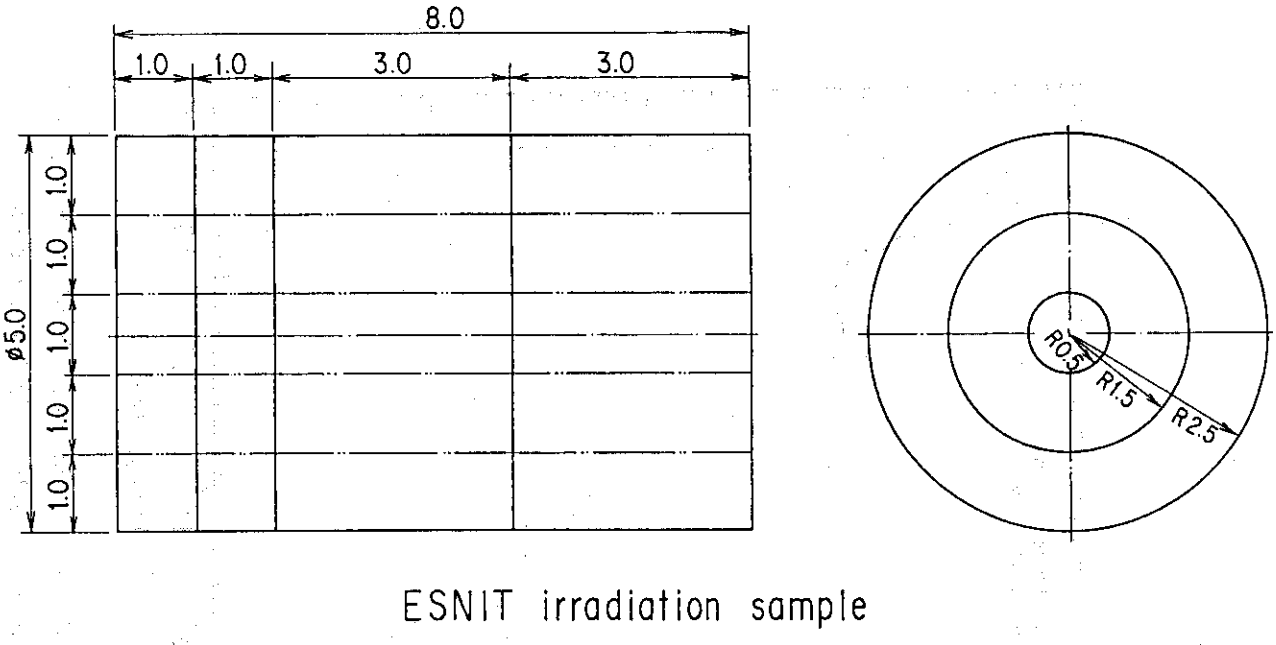

Fig. 4.2 Cell division for flux estimation inside of sample.

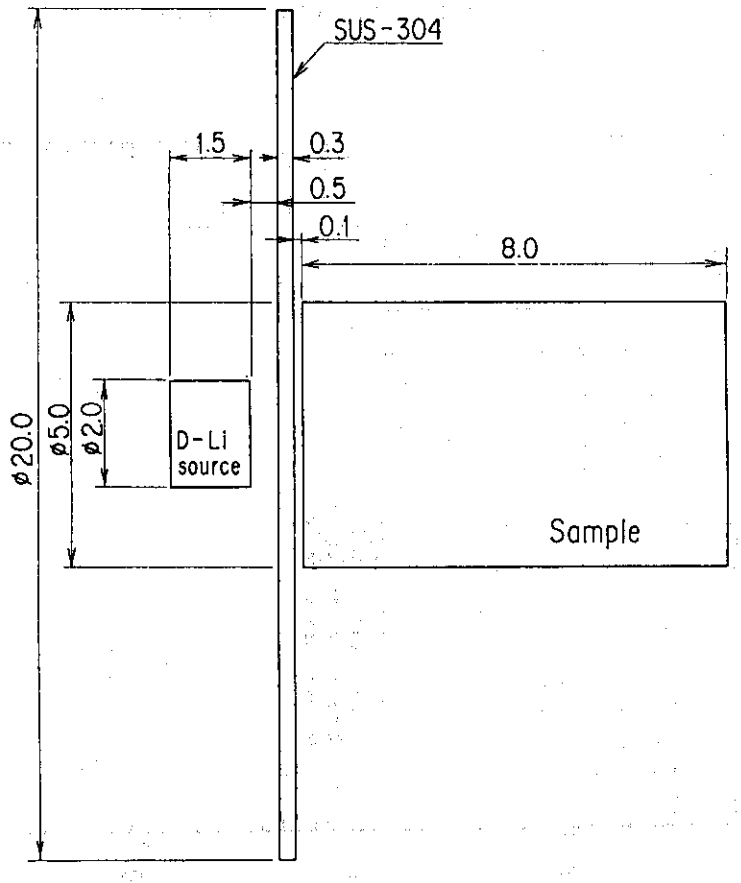

Fig. 4.3 Detail of model around the target.

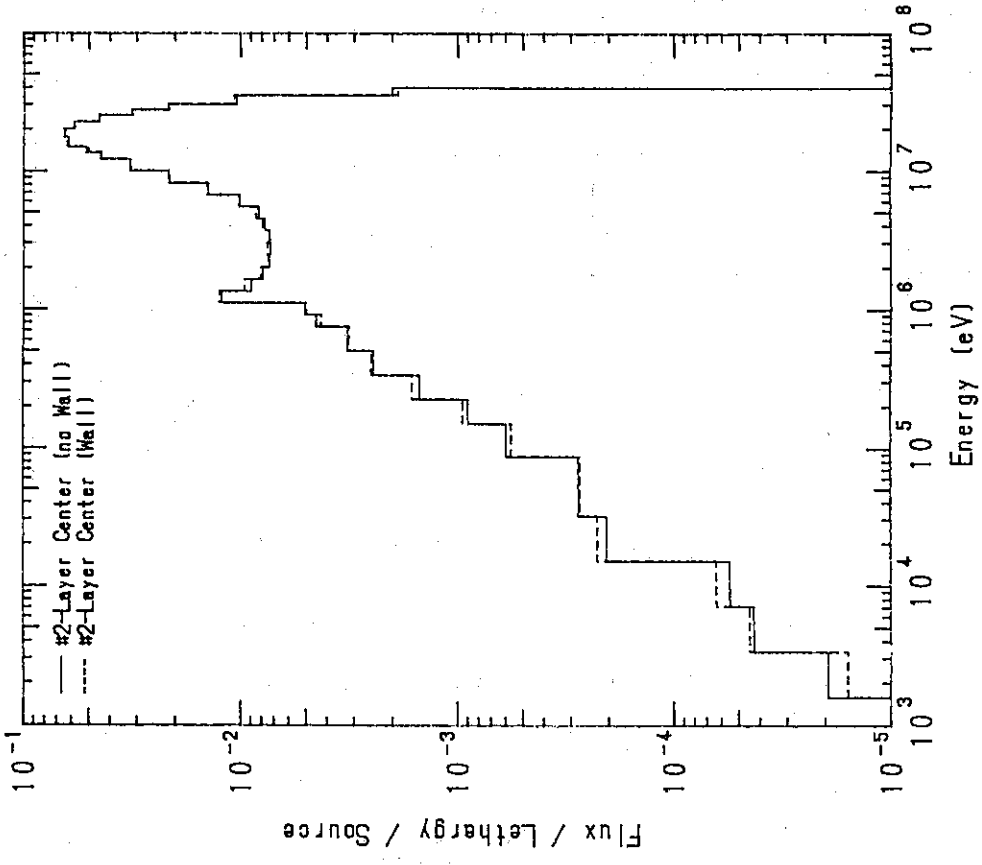

Fig. 4.4 Calculated spectra inside of the iron sample with and without the room wall for 40MeV deuterons.

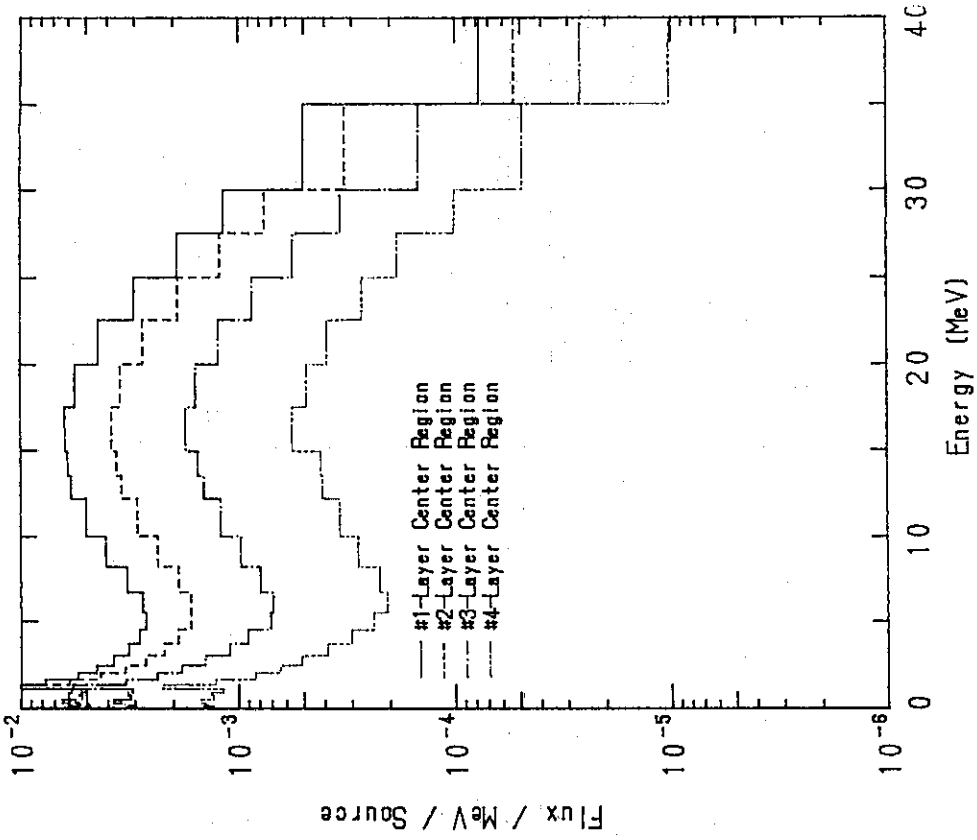

Fig. 4.5 Calculated spectra at various depths in iron for 40 MeV deuterons.

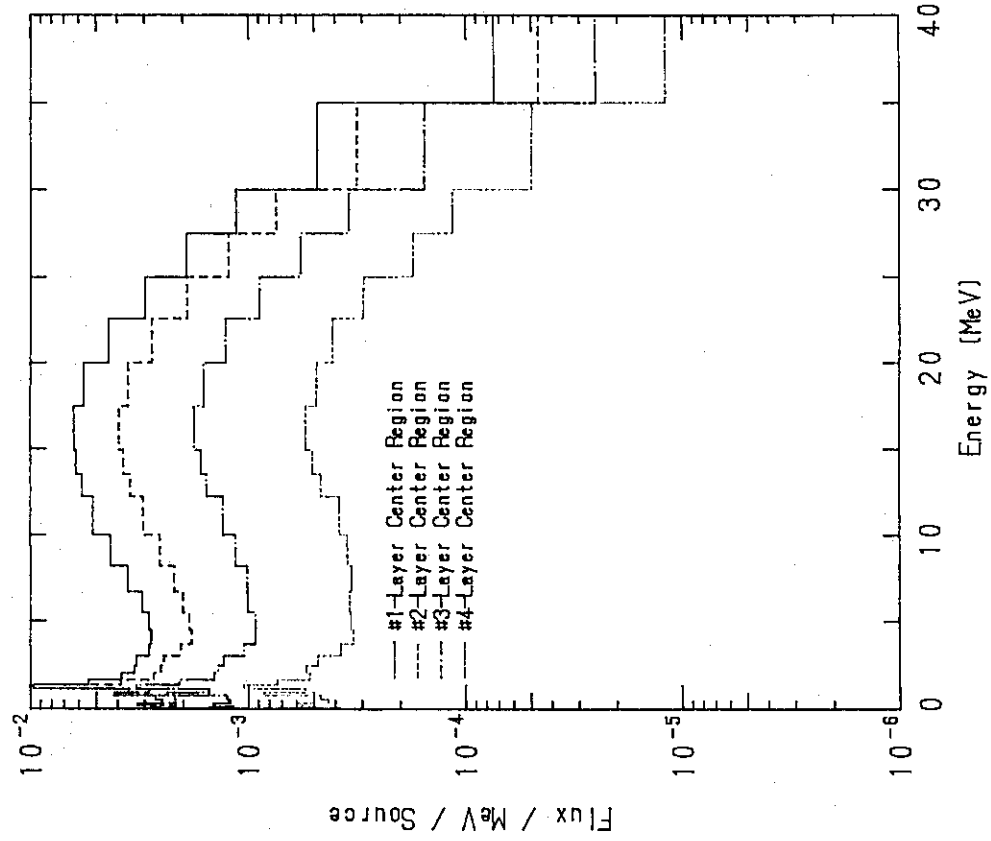

Fig. 4.6 Calculated spectra at various depths in alumina for 40 MeV deuterons.

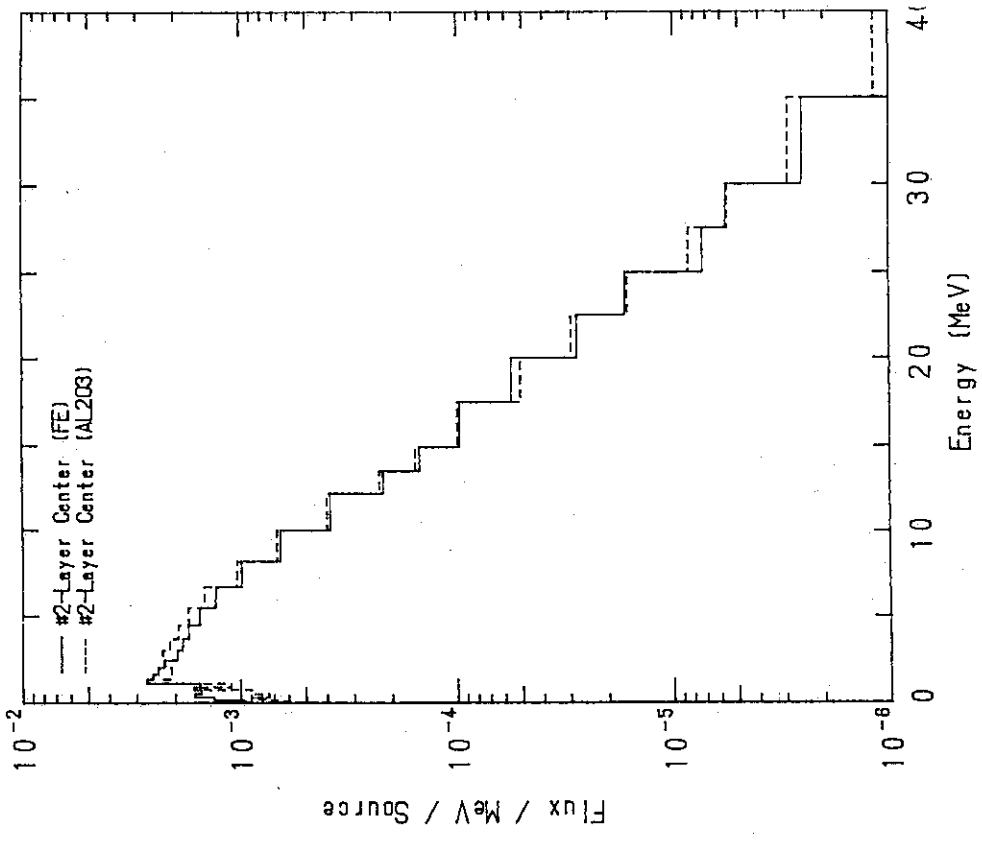

Fig. 4.7 Calculated spectra at 25mm depth in samples for 10 MeV deuterons.

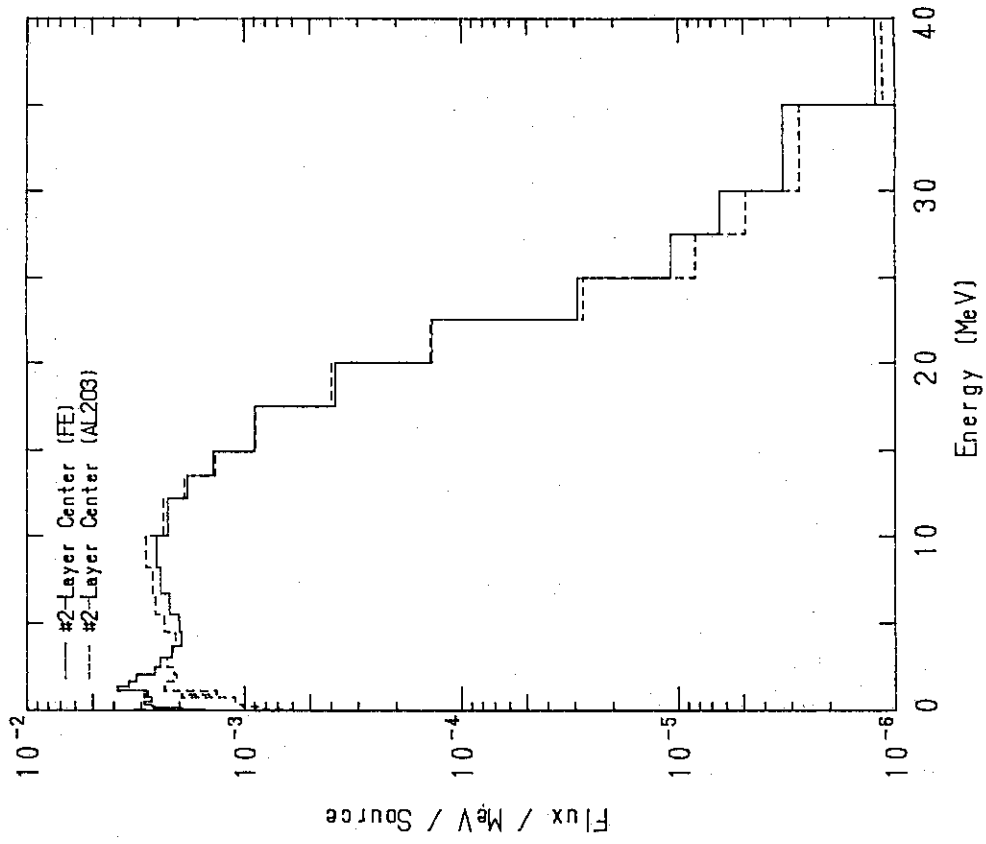

Fig. 4.8 Calculated spectra at 25mm depth in samples for 23 MeV deuterons.

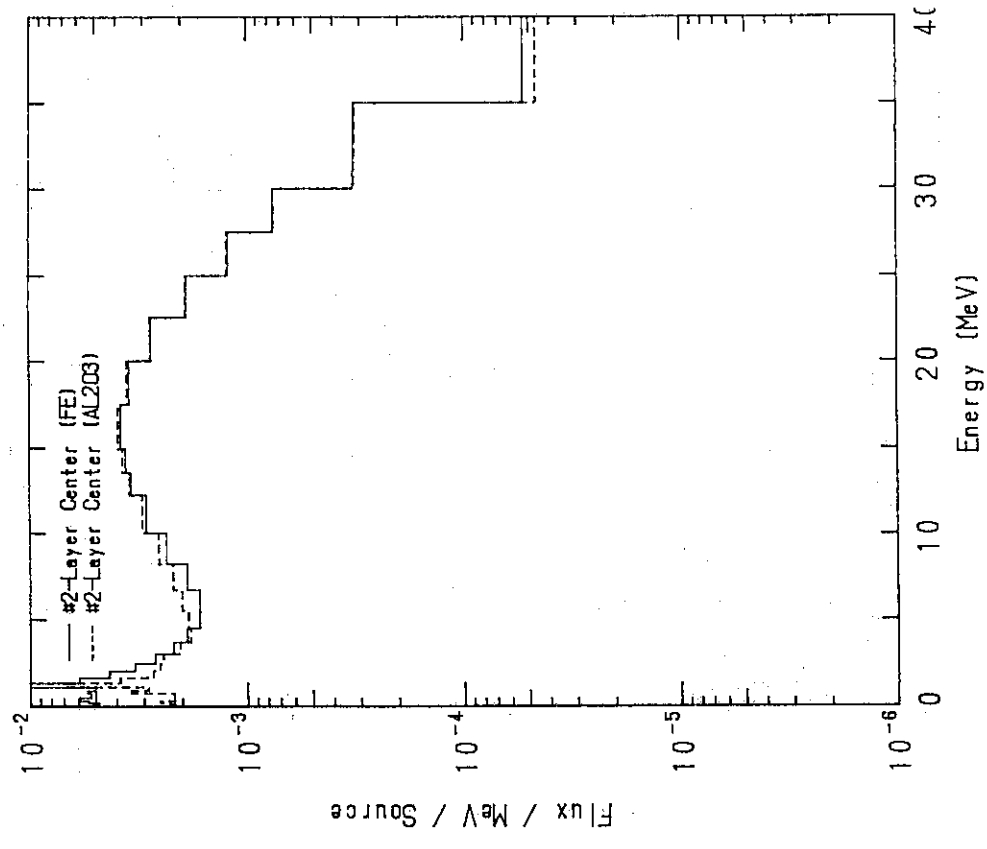

Fig. 4.9 Calculated spectra at 25mm depth in samples for 40 MeV deuterons.

5. CONCLUSIONS

The source model of thick lithium target for Li(d,n) reaction was formulated to calculate neutron field characteristics with the incident deuteron energies of 10-40 MeV. The calculations of the neutron flux spectrum distributions were also carried out near the lithium target. The neutron peak energy varied 4 to 15 MeV with the deuteron energy of 10 to 40 MeV. The neutron flux of 5 x 10^{13} to 1 x 10^{14} n/cm^2/s is achievable for the irradiation corresponding to the deuteron energy. The required irradiation volume of 125 cm^3 can also be obtained by the 40 MeV deuteron acceleration with 50 mA. The flux gradient requirement can not be satisfied by the ordinary beam profile but there is possibility by using a ring beam profile.

The present source model can be applied to the calculation of the neutron flux and damage parameters on the test specimens, and to the shielding design of the neutron irrdaiation facility. Using the present source model, the calculations of spectra including influences due to the test material itself and the irradiation cell wall were carried out for iron and alumina. From the results, the room returned neutrons do not affect much the spectrum inside of the test samples.

The calculations of damage parameter such as dpa, PKA and transmutation using the present spectra are also necessary. Through such calculations, the capability of ESNIT not only for material irradiation R&D in the scientific aspect but also for evaluation of the influence of high energy tail and for reduction of such influence by adopting the operation at the optimum peak energies, is expected to be exhibited. These calculations will be performed in the further studies.

ACKNOWLEDGMENTS

The authors wish to express their thanks to the members of the JAERI Accelerator Neutron Source Subcommittee, and especially to Drs. K. Noda, T. Kondo and H. Ohno of JAERI for their helpful discussion and comments. They also thank Dr. M. Nakagawa for his careful reading of this manuscript.

5. CONCLUSIONS

The source model of thick lithium target for Li(d,n) reaction was formulated to calculate neutron field characteristics with the incident deuteron energies of 10-40 MeV. The calculations of the neutron flux spectrum distributions were also carried out near the lithium target. The neutron peak energy varied 4 to 15 MeV with the deuteron energy of 10 to 40 MeV. The neutron flux of 5 x 10^{13} to 1 x 10^{14} n/cm^2/s is achievable for the irradiation corresponding to the deuteron energy. The required irradiation volume of 125 cm^3 can also be obtained by the 40 MeV deuteron acceleration with 50 mA. The flux gradient requirement can not be satisfied by the ordinary beam profile but there is possibility by using a ring beam profile.

The present source model can be applied to the calculation of the neutron flux and damage parameters on the test specimens, and to the shielding design of the neutron irrdaiation facility. Using the present source model, the calculations of spectra including influences due to the test material itself and the irradiation cell wall were carried out for iron and alumina. From the results, the room returned neutrons do not affect much the spectrum inside of the test samples.

The calculations of damage parameter such as dpa, PKA and transmutation using the present spectra are also necessary. Through such calculations, the capability of ESNIT not only for material irradiation R&D in the scientific aspect but also for evaluation of the influence of high energy tail and for reduction of such influence by adopting the operation at the optimum peak energies, is expected to be exhibited. These calculations will be performed in the further studies.

ACKNOWLEDGMENTS

The authors wish to express their thanks to the members of the JAERI Accelerator Neutron Source Subcommittee, and especially to Drs. K. Noda, T. Kondo and H. Ohno of JAERI for their helpful discussion and comments. They also thank Dr. M. Nakagawa for his careful reading of this manuscript.

REFERENCES

(1) Noda K., Oyama Y., Yamaguchi S., Maekawa H. and Hishinuma A.: J. Nucl. Materials, 174, 319 (1990).

(2) Noda K.,Matsuo H., Watanabe K., Sugimoto M., Kato Y., Sakai H., Oyama Y., Ohno H. and Kondo T.: J. Nucl. Materials, 179-181, 1147 (1991).

(3) Grand P., Batchelor K., Blewwett J. P., Goland A., Gurinsky D., Kukkonen J. and Snead C. L., Jr.: Nucl. Technol., 29, 327 (1976)

(4) Johnson D. L., Mann F. M., Watson J.W., Ullmann J. and Wyckoff W. G.: J. Nucl. Materials, 85 & 86, 467 (1979)

(5) Serber R.: Phys. Rev., 72, 1008 (1947)

(6) Lone M. A., Bigham C. B., Fraser J. S., Schneider H. R., Alexander T. K., Ferguson A. J. and McDonald A. B.: Nucl. Instrum. Methods, 143, 331 (1977)

(7) Weaver K. A., Anderson J. D., Barschall H. H. and Davis J. C.: Nucl. Sci. Eng., 52, 35 (1973)

(8) GolandA. N., Snead C. L. Jr., Parkin D. M. and Theus R. B.: IEEE Trans. on Nucl. Sci., NS-22, 1776 (1975)

(9) Lone M. A. and Bigham C. B.:" Neutron Source for Basic Physics and Application," Chapter VI, OECD/NEA report, p.140 (1983)

(10) Anderson H. M. and Ziegler J. F.:"Hydrogen Stopping Power and Ranges in All Elements," Pergamon (1977)

(11) Emmett M.B.:" The MORSE Monte Carlo Radiation Transport Code System," ORNL-4972, Oak Ridge National Laboratory (1975).

(12) Alsmiller R. G. Jr., Barish J.: " Neutron-Photon Multigroup Cross Sections for Neutron Energies ≤ 400MeV," ORNL/TM-7818, Oak Ridge National Laboratory (1981).

APPENDIX 1 : Jacobian in Relativistic Kinematics

The Jacobian used in Eq. (1) in the text is obtained from the following relations of relativistic kinematics. As illustrated in the Fig. A.1.1, the neutron energy and angle in the center of mass system are written by the energy and angle in the laboratory system, and the Jacobian is derived from those derivatives as follows:

$$E_{nC} = \gamma\left(E_{nL} - \beta\sqrt{E_{nL}^2 - M_n^2}\cos\theta_L\right) \tag{A.1}$$

and

$$\cos\theta_{nC} = \gamma\left(\cos\theta_{nL} - \frac{\beta}{\beta_{nL}}\right)\left(\gamma^2\left(\cos\theta_{nL} - \frac{\beta}{\beta_{nL}}\right)^2 + \sin^2\theta_{nL}\right)^{-\frac{1}{2}} \tag{A.2}$$

where $\beta_{nL} = \sqrt{1 - \left(\frac{M_n}{E_{nL}}\right)^2}$ and $\beta = \frac{\sqrt{E_{dL}^2 - M_d^2}}{E_{dL} + M_{Li}}$.

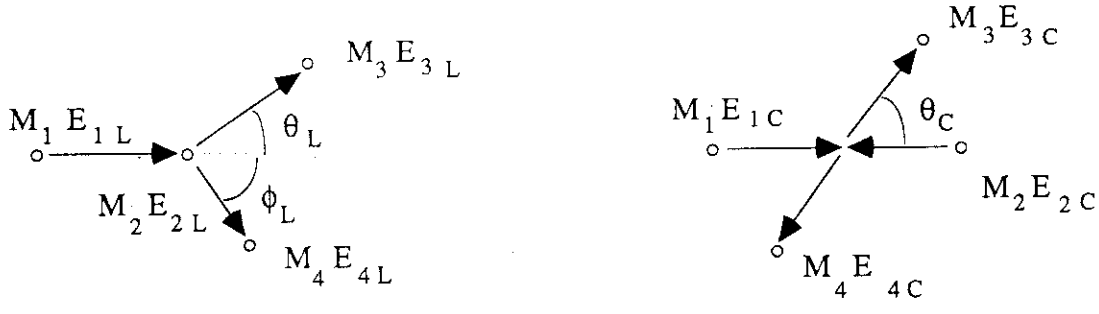

Laboratory System (Lab.) Center of Mass System (C.M.)

Fig. A.1.1 Definition of energy and mass. Here the numbers correspond to 1=deuteron, 2=lithium, 3=neutron and 4=beryllium. And E_L and E_C are energies in Lab. and in C.M. systems, respectively.

Then, the Jacobian is, dropping the index of neutron,

$$J = \left| \frac{\partial(E_C, \cos\theta_C)}{\partial(E_L, \cos\theta_L)} \right|$$

$$= \left| \frac{\partial E_C}{\partial E_L} \cdot \frac{\partial(\cos\theta_C)}{\partial(\cos\theta_L)} - \frac{\partial E_C}{\partial(\cos\theta_L)} \cdot \frac{\partial(\cos\theta_C)}{\partial E_L} \right| \quad . \tag{A.3}$$

Each derivative is obtained from the differentiation of equations (A.1) and (A.2). For neutron,

$$\frac{\partial E_C}{\partial E_L} = \gamma\left(1 - \frac{\beta}{\beta_L}\cos\theta_L\right) , \tag{A.4}$$

$$\frac{\partial E_C}{\partial(\cos\theta_L)} = -\gamma\beta\beta_L E_L , \tag{A.5}$$

$$\frac{\partial(\cos\theta_C)}{\partial(\cos\theta_L)} = \gamma A^{-3/2}\left(1 - \frac{\beta}{\beta_L}\cos\theta_L\right) , \tag{A.6}$$

$$\frac{\partial(\cos\theta_C)}{\partial E_L} = \frac{\gamma\beta M_n^2}{(\beta_L E_L)^3} \cdot A^{-3/2}\left(1 - \cos^2\theta_L\right) , \tag{A.7}$$

where $A = \gamma^2\left(\cos\theta_L - \frac{\beta}{\beta_L}\right)^2 + \sin^2\theta_L$. From Eqs. (A.4) to (A.7), the Jacobian can be written as:

$$J = \gamma^2 A^{-3/2}\left\{\left(\beta\cos\theta_L - \frac{1}{\beta_L}\right)^2 + \left(1 - \beta^2\right)\left(1 - \frac{1}{\beta_L^2}\right)\right\} . \tag{A.8}$$

This value agrees with the classical formula of $J = \beta_L / \beta_C$ in the reference (Ohlsen G.G.: Nucl. Instrum. Meth. 37, 240 (1965)) at low energy limit.

APPENDIX 2: Spectra of the Collided and Uncollided Neutrons at the Iron Sample Location for Deuteron Energies of 10, 23 and 40 MeV.

The spectra of the collided and uncollided neutrons at the sample location are compared in Figs. A.2.1-3 for three deuteron energies. The figures are normalized to the 50 mA case. The spectra of the uncollided neutrons were calculated by Eq. (4) for 40 mm-diameter beam and the collided ones done by the method described in Sec. 4. Thus these are not direct comparison but still useful to understand the phenomena. The spectra of the collided neutrons are 3 times lower than the uncollided ones below 23 MeV, while the those of 40 MeV is a half of the collided neutrons. The peak energies of the collided neutrons are higher than those of the uncollided ones and there is a valley around 4 MeV excluding the 10 MeV case. The numerical data for these spectra are listed in Tables A.2.1-A.2.2.

Table A.2.1 Uncollided flux produced by deuterons with 10-40MeV and 50mA at 2.5cm.

Energy (MeV)	Ed=40 MeV	Ed=23 MeV	Ed=10 MeV
	(/MeV/cm^2/s)		
2.0000	1.2064e+13	5.6520e+12	1.6424e+12
4.0000	1.7862e+13	8.2085e+12	2.1432e+12
6.0000	2.1493e+13	9.6790e+12	1.9000e+12
8.0000	2.3720e+13	9.8670e+12	1.2880e+12
10.000	2.4945e+13	8.7975e+12	7.8805e+11
12.000	2.5269e+13	6.7130e+12	3.5471e+11
14.000	2.4350e+13	4.4751e+12	2.2037e+11
16.000	2.2390e+13	2.8776e+12	1.3400e+11
18.000	1.9390e+13	1.6944e+12	8.0235e+10
20.000	1.5669e+13	8.6130e+11	4.7486e+10
22.000	1.1798e+13	3.8201e+11	2.7852e+10
24.000	8.3200e+12	1.1990e+11	1.6219e+10
26.000	5.6710e+12	7.8780e+10	9.3885e+09
28.000	3.7012e+12	5.1540e+10	5.4070e+09
30.000	2.3194e+12	3.3598e+10	3.1000e+09
32.000	1.3575e+12	2.1832e+10	1.7703e+09
34.000	6.7500e+11	1.4148e+10	1.0073e+09
36.000	1.4961e+11	9.1465e+09	5.7125e+08
38.000	1.5456e+10	5.9000e+09	3.2296e+08
40.000	1.0459e+10	3.7987e+09	1.8207e+08
Total>2MeV	4.7026e+14	1.1344e+14	1.5686e+13

Table A.2.2 Collided flux in Layer #2 of iron by deuterons with 10-40 MeV and 50mA at 2.5cm (MORSE-CG/DLC87)

Energy Boundary (MeV)	Mid-Energy (MeV)	Ed=40 MeV (/MeV/cm^2/s)	Ed=23 MeV	Ed=10 MeV
40.000	37.500	1.6155e+11	1.5830e+09	2.4797e+08
35.000	32.500	9.7550e+11	4.2622e+09	6.0827e+08
30.000	28.750	2.2732e+12	8.3069e+09	1.4065e+09
27.500	26.250	3.6529e+12	1.3969e+10	1.8585e+09
25.000	23.750	5.7136e+12	3.7623e+10	3.7056e+09
22.500	21.250	8.3083e+12	1.7586e+11	6.5222e+09
20.000	18.750	1.0529e+13	4.9090e+11	1.2800e+10
17.500	16.200	1.1565e+13	1.1503e+12	2.3131e+10
14.900	14.200	1.0923e+13	1.7788e+12	3.5232e+10
13.500	12.850	1.0366e+13	2.3420e+12	5.2179e+10
12.200	11.100	8.7989e+12	2.8965e+12	9.0087e+10
10.000	9.0950	7.1158e+12	3.2660e+12	1.5377e+11
8.1900	7.4450	5.7157e+12	3.1105e+12	2.3248e+11
6.7000	6.0950	5.0078e+12	2.8353e+12	3.1092e+11
5.4900	4.9900	5.0199e+12	2.5649e+12	3.6593e+11
4.4900	4.0850	5.7294e+12	2.5032e+12	4.1226e+11
3.6800	3.3450	6.6534e+12	2.7932e+12	4.3570e+11
3.0100	2.7350	8.1189e+12	3.1595e+12	4.6600e+11
2.4600	2.2400	1.0023e+13	3.3336e+12	5.3559e+11
2.0200	1.8350	1.3115e+13	4.0345e+12	5.6198e+11
1.6500	1.5000	1.8093e+13	4.3840e+12	6.0132e+11
1.3500	1.2300	3.0288e+13	4.9427e+12	6.4383e+11
1.1100	1.0085	1.5236e+13	3.5887e+12	3.6997e+11
0.90700	0.82500	1.6558e+13	3.7317e+12	3.8939e+11
0.74300	0.62050	1.5872e+13	3.4425e+12	3.4572e+11
0.49800	0.41600	1.7990e+13	3.7287e+12	3.8072e+11
0.33400	0.27900	1.6425e+13	3.4486e+12	3.2209e+11
0.22400	0.18700	1.4666e+13	3.3555e+12	3.1165e+11
0.15000	0.11825	1.5594e+13	2.5466e+12	2.2865e+11
0.086500	0.059150	1.5336e+13	1.9912e+12	2.3407e+11
0.031800	0.023400	2.7769e+13	4.1686e+12	3.5024e+11
0.015000	0.011050	1.5750e+13	3.4907e+12	1.5141e+11
0.0071000	0.0052250	2.5865e+13	3.1039e+12	3.6404e+11
0.0033500	0.0024650	2.4847e+13	1.3199e+12	1.1526e+11
0.0015800	0.0030600	2.2784e+13	9.6334e+11	3.2701e+11
0.0045400	0.0027750	5.0596e+12	0.0000	5.2949e+09
0.0010100	0.00061800	1.0005e+14	0.0000	0.0000
0.00022600				

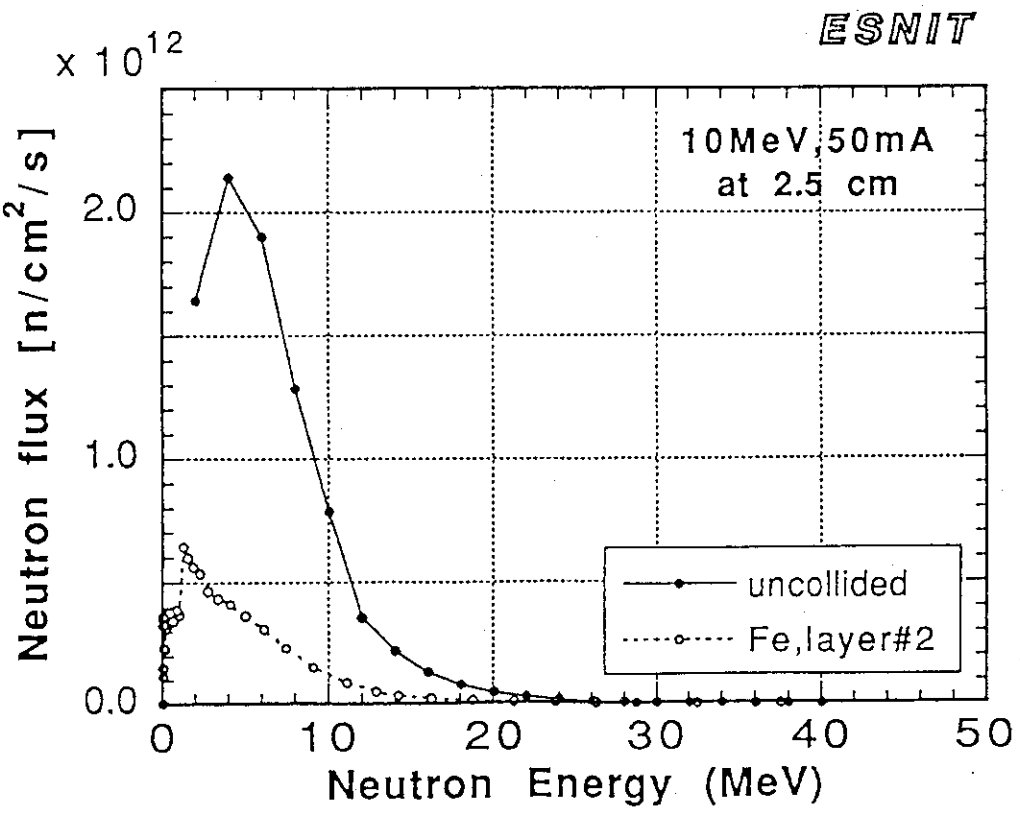

Fig.A.2.1 Comparison of the uncollided and collided neutron spectra at 25 mm depth in iron sample for 10 MeV deuterons.

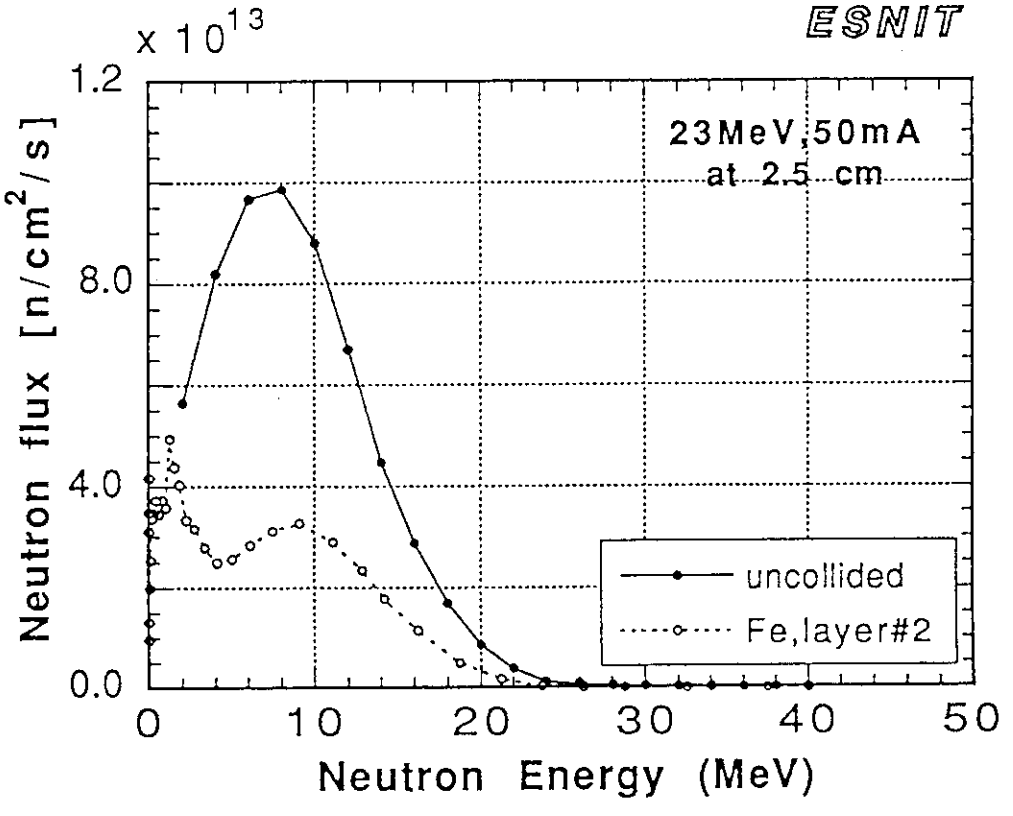

FIg.A.2.3 Comparison of the uncollided and collided neutron spectra at 25 mm depth in iron sample for 23 MeV deuterons.

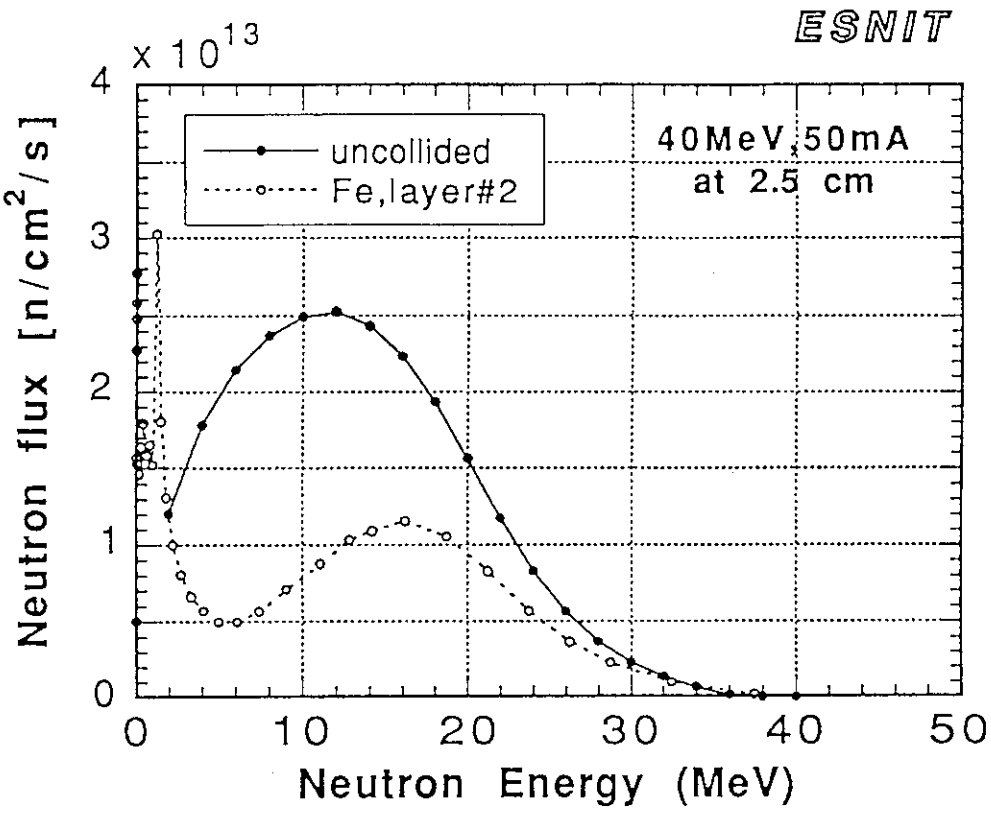

FIg.A.2.3 Comparison of the uncollided and collided neutron spectra at 25 mm depth in iron sample for 40 MeV deuterons.

APPENDIX 3

Program List for Calculation of the Neutron Flux Distribution

This program is written in command-file based on FORTRAN77 in VAX/VMS computer system.

```
$!-------------------------------------------------------------------------------
$                CRE FLX.FOR
C           FLX MAP CALCULATION
C-------------------------------------------------------------------------------
C -----------------------------------------------------------------------------
C     MAIN PROGRAM OF FLUX MAP CALCULATON
C           FOR D-LI SOURCE
C                BY Y. OYAMA  JAERI  AUGUST 31, 1989 -
C -----------------------------------------------------------------------------
C-------------------------------------------------------------------------------
C     ED0 = INCIDENT DEUTERON ENERGY (MEV)
C     DEN = NEUTRON ENERGY BIN ( MEV)
C     NMAX = NEUTRON BIN NUMBER
C     DX  = X-AXIS BIN ( CM)
C     DZ  = Z-AXIS BIN ( CM)
C     IXMAX= X BIN NUMBER
C     IZMAX= Z BIN NUMBER
C     D0  = THICKNESS OF LI LAYER (CM)
C     R0  = SOURCE RADIUS
C     W( ) = CURRENT PROFILE
C   DELTAE = DEUTERON ENRGY MESH FOR RANGE CALCULATION
C     DEV  = MESH FOR RANGE TO CALCULATE SOURCE DISTRIBUTION
C-------------------------------------------------------------------------------
    COMMON /DRANG/ ED0,DR(100),EDR(100),DRM(50),DELTAE,
   1             IRM,DEDR(100),DEV
    COMMON /SPACE/ X(100),Z(100),EN(100)
    COMMON /SOURCE/D0,R0,W(50),JRMAX,KPHM,A
```

```
C ==========< DATA INPUT >==========
C --------< DEUTERON & NEUTRON >----------
      DATA ED0,E0,DEN,NMAX/40.0,1.0,2.,20/
C --------< MAPPING REGION >----------
      DATA DX,IXMAX,DZ,IZMAX/0.5,5,0.5,10/
C --------< SOURCE REGION >----------
      DATA D0,R0/2.2,2.0/
      DATA JRMAX,KPHM,DELTAE,DEV/10,18,0.5,0.1/
      DATA CUR/0.05/
C------< NOMALIZATION >----------
C      ANORM=0.95/1.602E-16
CCC --- REVISED '91.12.17 ----------
      ANORM=1.335/1.602E-16
C----------
      DO 30 J=1,7
30    W(J)=1.0
      DO 31 J=8,JRMAX
31    W(J)=1.0
C ----------
C      READ(1,100) ED0,E0,DEN,NMAX
      READ(1,*) ED0
C      READ(1,101) DX,IXMAX,DZ,IZMAX
100    FORMAT(3E12.4,I6)
101    FORMAT(2(E12.5,I6))
1004   FORMAT(2X,I3,2X,F10.4)
      WRITE(6,1000) ED0,DEN,NMAX,ANORM
      WRITE(6,1001) DX,IXMAX,DZ,IZMAX
      WRITE(6,1002) D0,R0,JRMAX,KPHM,DEV
      WRITE(6,1004) (J,W(J),J=1,JRMAX)
1000  FORMAT(//5X,'ED0 (MEV) = ',F10.2,2X,'NEUTRON BIN (MEV) = ',
     1    F10.2/2X,'NEUTRON BIN NUMBER =',I3,2X,'NORM=',1PE12.5)
1001   FORMAT(/5X,'X-MESH (CM) = ',F10.4,2X,'X-BIN NUMBER = ',I4,
     1    2X,'Z-MESH (CM) = ',F10.4,2X,'Z-BIN NUMBER = ',I4)
1002   FORMAT(/5X,'TARGET THICKNESS (CM) = ',F10.4,2X,
     1    'TARGET RADIUS (CM) = ',F10.4,'TARGET RADIUS BIN = ',
     2    I4/5X,'PSI ANGLE BIN = ',I4,2X,'TARGET THICKNESS MESH = ',
     3    F10.4///)
```

```
C ------------------------------------------------------------------------------
      CALL DRANGG
C ------------------------------------------------------------------------------
      DO 6 I=1,IXMAX+1
      DO 6 J=1,IZMAX+1
      S(I,J)=0.0
6     CONTINUE
C --------< MAPPING REGION LOOP >-------------------------------------------------
      DO 1 I=1,IXMAX+1
      DO 2 J=1,IZMAX+1
      DO 3 K=1,NMAX
      EN(K)=K*DEN
      X(I)=(I-1)*DX
      Z(J)=(J-1)*DZ
      ENN=EN(K)
      XX=X(I)
      ZZ=Z(J)
C ------------------------------------------------------------------------------
      CALL FLX(XX,ZZ,ENN,FLXX)
C ------------------------------------------------------------------------------
      FLUX(I,J,K)=FLXX/A*ANORM
      S(I,J)=S(I,J)+FLUX(I,J,K)
CHECK  WRITE(6,2000) I,J,K,FLXX,S(I,J)
2000   FORMAT(2X,'I=',I3,'J=',I3,'K=',I3,'FLXX =',E12.5,
     1      2X,'S(I,J)=',E12.5)
3     CONTINUE
      S(I,J)=S(I,J)-(FLUX(I,J,1)+FLUX(I,J,NMAX))/2.
      S(I,J)=S(I,J)*DEN
2     CONTINUE
1     CONTINUE
C -------------< LOOP END >-----------------------------------------------------
      WRITE(6,300) ED0
300   FORMAT(1H1,2X,'INCIDENT DEUTERON ENERGY (ED0) =',
     1      1PE11.4,' [MEV]'/)
      WRITE(6,203)
      WRITE(6,200) (EN(K),K=1,NMAX)
      DO 4 I=1,IXMAX+1
      WRITE(6,201) I,X(I)
```

```
      DO 5 J=1,IZMAX+1
      WRITE(6,202) J,Z(J)
CHECK  WRITE(6,203)
CHECK  WRITE(6,200) (EN(K),K=1,NMAX)
      WRITE(6,204)
      WRITE(6,200) (FLUX(I,J,K),K=1,NMAX)
      WRITE(6,205) S(I,J)
205    FORMAT(2X,' FLUX SUM (>2 MEV) =',1PE12.4)
200    FORMAT(2X,1PE11.4,7E11.4)
201    FORMAT(//1X,'<<I=',I3,'>>',2X,' X (CM) =',1PE12.4)
202    FORMAT(/1X,'<J=',I3,'>',2X,' Z (CM) =',1PE12.4)
203    FORMAT(2X,' ** NEUTRON ENERGY **')
204    FORMAT(2X,' ** NEUTRON FLUX **')
5      CONTINUE
4      CONTINUE
      WRITE(6,213) CUR
213    FORMAT(1H1/2X,'DEUTERON CURRENT =',F10.4,' [A]')
      WRITE(6,212) (X(I),I=1,IXMAX+1)
212    FORMAT(2X,' X POSITION (CM): ',8F10.1)
      IZZ=INT((IZMAX+1)/8.0+1.0)
      DO 7 L=1,IZZ
      IKM1=(L-1)*8+1
      IKM2=L*8
      WRITE(6,211) (Z(J),J=IKM1,IKM2)
      DO I=1,IXMAX+1
      WRITE(6,222) (S(I,J)*CUR,J=IKM1,IKM2)
      ENDDO
211    FORMAT(2X,'Z POSITION (CM) =',8F5.1)
222    FORMAT(2X,17X,1P8E10.3)
7      CONTINUE
      STOP
      END
C=======================================================
C     SUBROUTINE DRANG ==> (ED0,DR,EDR,DRM)
C                    DEUTERON DEPTH VS. DEUTERON ENERGY
C                                        BY Y. OYAMA    28 AUG. '89
C-------------------------------------------------------------------------------
      SUBROUTINE DRANGG
```

```
      COMMON /DRANG/ ED0,DR(100),EDR(100),DRM(50),DELTAE,
     1        IRM,DEDR(100),DEV
      COMMON /SPACE/ X(100),Z(100),EN(100)
      DIMENSION E(100),R(100),S(100)
C     ED0=35.
C     DELTAE=0.5
      IM=INT(ED0/DELTAE)
      AM1=2.014102*931.4812
      DO 1 I=1,IM
      E(I)=ED0-(I-1)*DELTAE
      EDD=E(I)*1000*0.5
      B1=SQRT(E(I)**2+2.*E(I)*AM1)/(E(I)+AM1)
      B2=-0.5831+0.562*LOG(EDD)-0.1183*LOG(EDD)**2
     1 +0.009298*LOG(EDD)**3-0.000166*LOG(EDD)**4
      DEDX=(0.00153/B1**2)*(LOG(21470.*B1**2/(1-B1**2))-B1**2-B2)
      S(I)=1./DEDX
1     CONTINUE
      S(IM+1)=0.0
      DO 2 K=1,IM
      R(K)=0.0
2     CONTINUE
      DO 3 K=1,IM
      DO 4 J=1,K
      R(K)=R(K)+0.5*(S(J)+S(J+1))*DELTAE
4     CONTINUE
3     CONTINUE
      DO 6 K=1,IM
      R(K)=R(K)/(0.5297/7.*6.022*100)
6     CONTINUE
      WRITE(6,101)
101    FORMAT(1X,'NO.',5X,' ED0 - ED(MEV) ',5X,'DEPTH(CM)')
      DO 7 K=1,IM
      WRITE(6,100) K,ED0,E(K+1),R(K)
100    FORMAT(2X,I2,2X,1PE12.4,2X,E12.4,2X,E12.4)
7     CONTINUE
C     DEV=0.05
      IRM=INT(R(IM)/DEV)+1
      R(0)=0.0
```

```
      DO 8 I=1,IRM+1
      DR(I)=(I-1)*DEV
 8    CONTINUE
      DO 21 I=1,IRM+1
      DO 20 K=1,IM
      IF(R(K).GT.DR(I)) THEN
      EDR(I)=(E(K+1)-E(K))*(DR(I)-R(K-1))/(R(K)-R(K-1))+E(K)
      GO TO 21
      ELSE
      GO TO 20
      ENDIF
 20   CONTINUE
 21   CONTINUE
      DO 22 I=1,IRM
      DEDR(I)=EDR(I)-EDR(I+1)
 22   CONTINUE
      DO 23 J=1,IRM+1
      K=INT(J/2)
      DRM(K)=DR(J)
 23   CONTINUE
      WRITE(6,103)
 103  FORMAT(/2X,'NO.',2X,'DR(CM)',6X,'EDR(MEV)')
      WRITE(6,102) (K,DR(K),EDR(K),K=1,IRM+1)
 102  FORMAT(2X,I2,2X,1PE12.4,2X,E12.5)
      RETURN
      END
C-------------------------------------------------------------------------------
C     SUBROUTINE FLX
C-------------------------------------------------------------------------------
      SUBROUTINE FLX(X,Z,EN,FLXX)
      COMMON /DRANG/ ED0,DR(100),EDR(100),DRM(50),DELTAE,
     1       IRM,DEDR(100),DEV
C     COMMON /SPACE/ X(100),Z(100),EN(100)
      COMMON /SOURCE/D0,R0,W(50),JRMAX,KPHM,A
C     DIMENSION SS(50,50,200),R(50),PH(200)
      DIMENSION R(50),PH(200)
      DRR=R0/JRMAX
      DPH=2*3.14159/KPHM
```

```
      DO 51 J=1,JRMAX+1
      R(J)=(J-1)*DRR
C     W(J)=1.0
51    CONTINUE
      A=0.0
      DO 55 J=1,JRMAX
      A=A+3.14159*(R(J+1)**2-R(J)**2)*W(J)
55    CONTINUE
      DO 52 K=1,KPHM+1
      PH(K)=(K-1)*DPH
52    CONTINUE
      G1=0.0
C     DO 1 I=1,INT((IRM+1)/2)
C--------< SOURCE REGION LOOP >-----------------------------------------------
      DO 1 I=1,IRM
      DO 2 J=1,JRMAX
      DO 3 K=1,KPHM
      RL=(Z+D0-DR(I))**2+(X-R(J)*COS(PH(K)))**2
     1 +(R(J)*SIN(PH(K)))**2
      RL=SQRT(RL)
      TH=ACOS((Z+D0-DR(I))/RL)
      DO 3 K=1,KPHM
      RL=(Z+D0-DR(I))**2+(X-R(J)*COS(PH(K)))**2
     1 +(R(J)*SIN(PH(K)))**2
      RL=SQRT(RL)
      TH=ACOS((Z+D0-DR(I))/RL)
      ED=EDR(I)
      DED=DEDR(I)
CHECK  WRITE(6,200) I,J,K,RL,TH,EN
200   FORMAT(2X,'I=',I3,'J=',I3,'K=',I3,'RL=',E12.5,
     1 ' TH=',E12.5,' EN=',E12.5)
C-------------------------------------------------------------------------------
      CALL DLI(TH,ED,EN,G)
C-------------------------------------------------------------------------------
      G1=G1+G*W(J)*R(J)*DRR*DPH*DED/RL**2
3     CONTINUE
2     CONTINUE
1     CONTINUE
```

```
C ---------< SOURCE REGION LOOP END >-----------------------------------------------
      FLXX=G1
CHECK   WRITE(6,1000) FLXX
1000    FORMAT(2X,'FLXX=',E12.5)
      RETURN
      END
C-------------------------------------------------------------------------------
      SUBROUTINE DLI(TH,ED,EN,G)
C===============================================================
C      D-LI REACTION NEUTRON PRODUCTION
C-------------------------------------------------------------------------------
C                    DLI.FOR
C                              1989.7.5 -
C
C       Calculation of Energy and Angular Distribution of Neutrons
C             Produced by 7-Li(d,n)Be-8 Reaction
C
C   Cross Section : R.Serber : Phys. Rev. 72 (1947) 1008
C                   D.L.Johnson and F.M.Mann : J.Nucl.Materials,
C                   85&86 (1979) 467
C   Stopping Power: H.M.Andersen and J.F.Ziegler : Hydrogen Stopping
C                   Power and Ranges in All Elements, Pergamon (1977)
C-------------------< DIFINITIONS >-----------------------------------------------
C   KMAX  = Incident Deuteron Energy [MeV]
C      DIMENSION SUM(20),F1(0,100),F2(20,50,100),
C     * G1(20,100),G2(20,100),G(20,100),EDCT(20)
C   KMAX  = Incident Deuteron Energy [MeV]
C   ED,K  = Deuteron Energy [MeV] in Lab-System
C   EDC   = Deuteron Energy [MeV] in CM-System
C   EN,J  = Emitted Neutron Energy [MeV] in Lab-System
C   ENC   = Emitted Neutron Energy [MeV] in CM System
C   TH    = Neutron Emission Angle [Degree] in Lab-System
C   THR   = Neutron Emission Angle [Radian] in Lab-System
C   THC   = Neutron Emission Angle [Degree] in CM-System
C -------------------------------------------------------------------------------
      COMMON /DRANG/ ED0,DR(100),EDR(100),DRM(50),DELTAE,
     1       IRM,DEDR(100),DEV
      COMMON /SOURCE/D0,R0,W(50),JRMAX,KPHM,A
```

```
      DIMENSION EDCT(20)
      REAL   IEDX1
C ---------------<DEFAULT DATA>-----------------------------------------------------
     DATA KMAX,DELTAE,IEDX1,IEDX2/35,1.00,10,15/
     DATA IDTH,ITH1,EXM/15,0,45/
      DATA SIGS0,SIGS1,SIGC0/0.06,0.04,0.01/
     DATA ITEMP,IPRT2,IPRT6/0,1,0/
C ---------------------------------------------------------------------------------
      KMAX=ED
      NORM=1.0
      SIGC1=0.001
      SIGS2=0.05
C-------< LIMIT OF STRIPPING REACTION >-----------------------------------------
    KMIN1=INT(6./DELTAE)
C-------< LIMIT OF COMPOUND FORMATION >-----------------------------------------
C      KMIN2=INT(1.65/DELTAE)
      KMIN2=INT(1./DELTAE)
C---------------------------------------------------------------------------------
101   FORMAT(2I6)
102   FORMAT(2F6.3)
103   FORMAT(3I6)
CHECK     WRITE(6,601) KMAX,DELTAE,IEDX1,IEDX2,SIGS0,SIGC0,ITEMP
601   FORMAT(1H ,//,5X,'INCIDENT DEUTERON ENERGY =',I3,3X,'DE =',F6.2,
     * 3X,'EDX1 =',F3.0,3X,'EDX2 =',I3,/,5X,'SIGS0 =',F6.2,/,5X,
     *'SIGC0 =',F6.2,/,5X,'ITEMP =',I2,//)
C ----------< SET CONSTANT >---------------------------------------------------
      AMU=931.4812
      EB=2.23
      EDX1=IEDX1
      EDX2=IEDX2
      A1=2.014102
      A2=7.016000
      A3=1.007823
      A4=8.005305
      AM1=A1*AMU
      AM2=A2*AMU
      AM3=A3*AMU
      AM4=A4*AMU
```

```
      ALI=7.
      ACOMP=9.
      RAD=3.1415927/180.
      KMAXD=KMAX/DELTAE
      EDCT(1)=0.
      EDCT(2)=0.1000
      EDCT(3)=0.3590
      EDCT(4)=1.7339
      EDCT(5)=3.9984
      EDCT(6)=7.2014
C
      EDCT(7)=11.3839
      EDCT(8)=16.5819
      EDCT(9)=22.8274
      EDCT(10)=30.1496
C -----------------------------------------------------------------------------
      THR=TH
      COST=COS(THR)
      SINT=SIN(THR)
      TANT=TAN(THR)
C -----------------------------------------------------------------------------
      T3=EN
      BETA3=SQRT(T3**2+2.*T3*AM3)/(T3+AM3)
C
      EDCMAX=(KMAX*AM2+AM1**2+AM1*AM2)/SQRT(2*KMAX*AM2+(AM1+AM2)**2)-AM1
      EDD=ED*1000.*0.5
C ------< 1 TO 1000 MEV RANGE FORMULA OF STOPPING POWER >--------------
       B1=SQRT(ED**2+2.*ED*AM1)/(ED+AM1)
       B2=-0.5831+0.562*LOG(EDD)-0.1183*LOG(EDD)**2
     1  +0.009298*LOG(EDD)**3-0.000166*LOG(EDD)**4
       DEDX=(0.00153/B1**2)*(LOG(21470.*B1**2/(1-B1**2))-B1**2-B2)
C ----< RELATION OF RELATIVISTIC KINEMATICS >-----------------------------
      BETA=SQRT(ED**2+2.*ED*AM1)/(ED+AM1+AM2)
      BB=BETA/BETA3
      GAMMA=1./SQRT(1.-BETA**2)
      TANTC=SINT/GAMMA/(COST-BB)
      ENC=GAMMA*(EN+AM3-BETA*SQRT(EN**2+2.*EN*AM3)*COST)-AM3
```

```
      IF(TANTC.LT.0) THEN
      THC=3.14159-ATAN(TANTC)
       ELSE
      THC=ATAN(TANTC)
       ENDIF
     EDC=SQRT(2*ED*AM2+(AM1+AM2)**2)-(AM1+AM2)
      ED1=(EDC**2+2*EDC*AM2)/2/(AM1+AM2+EDC)
C-------------------------------------------------------------------------------
     BETA3C=SQRT(ENC**2+2.*ENC*AM3)/(ENC+AM3)
     R=BETA/BETA3C
     IF(R.LT.1) GO TO 2000
     THMAX=ATAN(1./GAMMA/SQRT(R**2-1.))
     IF(THR.GT.THMAX) GO TO 20
2000  CONTINUE
C ----< JACOBIAN (CLASSICAL) >-----------------------------------------------
C      DEDW=BETA3C/BETA3
C       DEDW=1./DEDW
C ----< JACOBIAN ( RELATIVISTIC) >-------------------------------------------
      AA=GAMMA**2*(COST-BETA/BETA3)**2+1-COST**2
      DJ1=GAMMA**2*(1-BETA/BETA3*COST)**2/AA**1.5
      DJ2=(GAMMA*BETA*AM3/BETA3/(T3+AM3))**2*(1-COST**2)/AA**1.5
       DEDW=DJ1+DJ2
C-------------------------------------------------------------------------------
     IF(EDC.GT.EDX1) GO TO 1000
       IF(EDC.LT.6) THEN
       SIGS=0.0
       ELSE
     SIGS=(SIGS0-SIGS1)*(EDC-6)/(EDX1-6)+SIGS1
       ENDIF
     GO TO 1001
1000  SIGS=SIGS0
1001  CONTINUE
     IF(EDC.GT.EDX2) GO TO 1100
1001  CONTINUE
     IF(EDC.GT.EDX2) GO TO 1100
     SIGC=(SIGC0-SIGC1)*(EDX2-EDC)/EDX2+SIGC1
     GO TO 1101
1100  SIGC=0.
```

```
1101  CONTINUE
C -------< C.M. FRAME CROSS SECTION WITH LAB.SYSTEM PARAMETER >---
      XS1=(ED1-EB)*EB
      XS21=((ENC-ED1*0.5)**2+EB*ED1)**1.5
C ------< ANGULAR TERM >-----------------------------------------------------------
      TH0=SQRT(EB/ED1)
      XS22=TH0/(TH0**2+THC**2)**1.5
C----< CORRECTION WITH QUASI-FREE SCATTERING CONTRIBUTION >-------
C----< NO USE BECAUSE OF SMALL EFFECT >---------------------------------------
C       S=0.22-0.002*ED1
C     XS22=TH0/(TH0**2+TANTC**2)**1.5*(1-S)+S*COSTC
C-----------------------------------------------------------------------------------
C ----< HIGH ENERGY TAIL CUT >-----------------------------------------------------
C      IF(ABS(ENC-ED1*0.5).GT.1*1.53*SQRT(EB*(EDCMAX-1.6-EB))) THEN
       IF((ED1-6.).GT.0) THEN
       IF(ABS(ENC-ED1*0.5).GT.2*SQRT(EB*(ED1-1.6-EB))) THEN
        XS=0.0
        ELSE
        XS=0.5*XS1/XS21*XS22
        ENDIF
       ELSE
        XS=0.5*XS1/XS21*XS22
       ENDIF
C ---< NUCLEAR TEMPERATURE (ACOMP=9 OF BE-9) >-------------------------------
      T=3.2*SQRT(EDC/ACOMP)
      IF(ITEMP.EQ.0) GO TO 3500
      L=0
3000  L=L+1
      IF(EDC.GT.EDCT(L)) GO TO 3000
      L1=L-1
      L2=L
     T=(FLOAT(L1)-1.)*0.5+(EDC-EDCT(L1))/(EDCT(L2)-EDCT(L1))*0.5
3500  CONTINUE
C ----< EVAPOLATION CROSS SECTION >-----------------------------------------
      XC=ENC*EXP(-ENC/T)
C -----------------------------------------------------------------------------
      F1=NORM*SIGS*XS/DEDX*DEDW
      F2=NORM*SIGC*XC/DEDX*DEDW
```

```
C ------------------------------------------------------------------------
      THMAX1=THMAX*180./3.14159
      THC1=THC*180./3.14159
CHECK     IF(I.EQ.7) WRITE(6,246) I,J,K,ED,EDC,BETA,BETA3,BETA3C,BB,R,
C     * THMAX1,THC1,ENC,XS,DWDW,DEDE,F1(I,J,K),F2(I,J,K)
C246   FORMAT(1H ,3I3,1P15E8.1)
CHECK
      G=F1+F2
       GO TO 10
20     G=0.0
10     CONTINUE
CHECK
C     IF(IPRT6.EQ.0) GO TO 4000
C    WRITE(6,600) (ITH(I),I=1,9)
C     DO 70 J=2,36
C     WRITE(6,603)  J,(G(I,J),I=1,9)
C70    CONTINUE
C     WRITE(6,602) (SUM(I),I=1,9)
C4000  CONTINUE
C     WRITE(2,200) (FLOAT(J),J=2,40)
C     WRITE(2,200)  (G(I0,J),J=2,40)
C     IF(IPRT2.EQ.0) GO TO 5000
C     WRITE(2,200) (FLOAT(J),J=2,40)
C     WRITE(2,200)   (G(2,J),J=2,40)
C     WRITE(2,200) (FLOAT(J),J=2,40)
C     WRITE(2,200)   (G(3,J),J=2,40)
C     WRITE(2,200) (FLOAT(J),J=2,40)
C     WRITE(2,200)   (G(4,J),J=2,40)
C     WRITE(2,200) (FLOAT(J),J=2,40)
C     WRITE(2,200)   (G(5,J),J=2,40)
C     WRITE(2,200) (FLOAT(J),J=2,40)
C     WRITE(2,200)   (G(6,J),J=2,40)
C     WRITE(2,200) (FLOAT(J),J=3,40)
C     WRITE(2,200)   (G(7,J),J=3,40)
C     WRITE(3,200)   (TH(I),I=1,20)
C     WRITE(3,200)   (SUM(I),I=1,20)
C5000  CONTINUE
C600   FORMAT(1H ,//,3X,'EN[MEV]',9I10,/)
```

```
C603   FORMAT(2X,I5,6X,1P9E10.2)
C602   FORMAT(1H ,/,5X,'SUM',5X,1P9E10.2,////)
C200   FORMAT(6E12.5)
C      IF(IPRT6.EQ.0) GO TO 999
C      DO 99 K=1,35
C      WRITE(6,654) K,F2(5,2,K),F2(5,3,K),F2(5,4,K),F2(5,7,K),
C     * F2(5,10,K),F2(5,13,K),F2(5,16,K),F2(5,19,K),
C     * F2(5,22,K),F2(5,25,K)
C654   FORMAT(1H ,I5,1P10E10.2)
C99    CONTINUE
C999   CONTINUE
CHECK
       RETURN
       END
$!=====< COMPILE $ LINK >=============================================
$!     FOR/LIS FLX.FOR
$      FOR  FLX.FOR
$      LINK FLX.OBJ
$!-------------------------------------------------------------------------------
$!     ASS/USER    FLX.DAT     FOR001          !INITIAL INPUT
$!     ASS/USER    LPA0:               FOR006          !OUTPUT DEVICE
$!     ASS/USER   FOR006.DAT           FOR006          !OUTPUT FILE
$!     RUN FLX                                         !EXECUTION
$!++++++< CLEAN UP FILES >+++++++++++++++++++++++++++++++++++++++++++++
$      DEL FLX.FOR;*
$      DEL FLX.OBJ;*
$!     DEL FLX.EXE;*
$      PUR FLX.EXE
$      PUR FLX.COM
$      PUR FLX1.COM
$!++++++++++< END >+++++++++++++++++++++++++++++++++++++++++++++++++++++
```